LUND UNIVERSITY

Cerebral intraventricular hemorrhage and post-hemorrhagic ventricular dilatation in preterm infants: new mechanistic insights and potential treatment strategies

Romantsik, Olga

2021

Cerebral intraventricular hemorrhage and post-hemorrhagic ventricular dilatation in preterm infants: new mechanistic insights and potential treatment strategies

OLGA ROMANTSIK
DEPARTMENT OF CLINICAL SCIENCES | FACULTY OF MEDICINE | LUND UNIVERSITY

Cerebral intraventricular hemorrhage and post-hemorrhagic ventricular dilatation in preterm infants: new mechanistic insights and potential treatment strategies

Cerebral intraventricular hemorrhage and post-hemorrhagic ventricular dilatation in preterm infants: new mechanistics insights and potential treatment strategies

Olga Romantsik

LUND
UNIVERSITY

DOCTORAL DISSERTATION
by due permission of the Faculty of Medicine, Lund University, Sweden.
To be defended at Segerfalksalen, BMC Sölvegatan 19, Lund.
Friday, March 26th at 9am.

Faculty opponent
Associate Professor Cora Nijboer
Division of Perinatology and Gynecology, University
Medical Center, Utrecht

Organization LUND UNIVERSITY	Document name DOCTORAL DISSERTATION
	Date of issue March 26, 2021
Author: Olga Romantsik	Sponsoring organization

Title and subtitle. Cerebral intraventricular hemorrhage and post-hemorrhagic ventricular dilatation in preterm infants: new mechanistic insights and potential treatment strategies

Abstract

Intraventricular hemorrhage (IVH) is one of the major co-morbidities of premature birth associated with post-hemorrhagic ventricular dilatation (PHVD) development, long-term neurodevelopmental impairment, behavioral problems, special educational needs, and dependency on social security.

Hypothesis and aims: We believe that extravasated blood and further release of extracellular hemoglobin (Hb) are crucial in brain injury following IVH and consequent development of PHVD. The overall goal of this project focuses on further pathogenetic insights of white and gray matter (GM) injury following IVH and the development of possible neuroprotective treatment strategies that may promote brain development in preterm infants.

Methods: *Paper I.* We characterized extracellular Hb distribution within periventricular white matter (WM) in preterm rabbit pups following IVH. *Paper II.* We evaluated the cerebral biodistribution and possible functional neuroprotection of intracerebroventricularly administered alpha-1-microglobulin (A1M), a heme and free radical scavenger, in preterm rabbit pups following IVH. *Paper III.* We conducted a comprehensive review of preclinical and clinical studies on WM injury following IVH. *Paper IV.* We evaluated high-frequency ultrasound (HFU) as a tool for the reconstruction of volumetric volume in preterm rabbit pups with PHVD and compared its accuracy and reliability with that of a gold-standard – magnetic resonance imaging (MRI). *Paper V.* We established a novel model of PHVD in preterm rabbit pups and characterized the survival, neurobehavior, WM, and GM injury, as well as altered corticogenesis.

Results: *Paper I.* Following IVH extracellular Hb was widely distributed throughout the brain WM, particularly in periventricular white matter areas with high extracellular plasticity following IVH. *Paper II.* Exogenous A1M (recombinant) was extensively distributed within brain WM with further extension into cerebellar WM following IVH. Moreover, A1M exhibited high co-existence with extracellular Hb. Administration of A1M (human) decreased pro-inflammatory and oxidative damage. *Paper III.* A wide range of animal models have been used to explore pathogenetic mechanisms of IVH and related brain damage; possible targets involved in enhancing brain damage have been identified. Nevertheless, the effectiveness of potential interventions is still limited. *Paper IV.* HFU-based volumetric reconstruction of brain ventricles is highly accurate and reliable as compared to MRI and may be a promising bed-side tool for evaluating of progression of PHVD in preterm infants. *Paper V.* IVH and PHVD lead to a long-term alteration of cortical myelination microstructure, disruption of cortical organization, selectively reduction in neurogenesis and synaptogenesis, reduction in parvalbumin-positive interneurons and their dysmaturation.

Conclusions: Extracellular Hb travels easily throughout brain WM following IVH and it may be one of the key factors for induction of brain damage by triggering pro-inflammatory and oxidative cascades. Furthermore, IVH, leading to PHVD, disrupts normal corticogenesis, alters myelinate microstructure, causes a selective reduction in neurons, interneurons, and synapses. A1M, as a heme and free radicals scavenger, may attenuate WM damage, confirming that extracellular Hb is causative in ongoing neuroinflammation following IVH. Thus, A1M may be a possible treatment strategy in preterm infants with IVH. HFU represents a highly accurate tool for volumetric reconstruction of ventricles for diagnosis and management of PHVD.

Key words: Preterm birth, IVH, PHVD, Extracellular Hb, A1M, animal IVH models, white matter injury, gray matter injury, HFU, MRI

Classification system and/or index terms (if any)

Recipient's notes	Number of pages 84	Price
	Security classification	

Signature *Romantsik*   Date 2021-02-18

Cerebral intraventricular hemorrhage and post-hemorrhagic ventricular dilatation in preterm infants: new mechanistics insights and potential treatment strategies

Olga Romantsik

LUND

UNIVERSITY

Coverphoto by Auguste Renoir "The Dancer",1874

Life is an opportunity, benefit from it.

Life is beauty, admire it.

Life is bliss, taste it.

Life is a dream, realize it.

Life is a challenge, meet it.

Life is a game, play it.

Life is costly, care for it.

Life is wealth, keep it.

Life is love, enjoy it.

Life is a mystery, know it.

Life is a promise, fulfill it.

Life is sorrow, overcome it.

Life is a song, sing it.

Life is a struggle, accept it.

Life is a tragedy, confront it.

Life is an adventure, dare it.

Life is too precious, do not destroy it.

Life is life, fight for it!

Mother Theresa of Calcutta

Table of Contents

Original papers

I. Ley D, **Romantsik O**, Vallius S, Sveindóttir K, Sveindóttir S, Agyemang AA, Baumgarten M, Mörgelin M, Lutay N, Bruschettini M, Holmquist B, Gram M. High presence of extracellular hemoglobin in periventricular white matter following preterm intraventricular hemorrhage. *Front Physiol 2016; 7:330.*

II. **Romantsik O**, Agyemang AA, Sveindóttir S, Rutardóttir S, Holmquist Bo, Cinthio M, Mörgelin M, Gulcin Gumus, Karlsson H, Hansson SR, Åkerström B, Ley D, Gram M. The heme and radical scavenger alpha-1-microglobulin (A1M) confers early protection of the immature brain following preterm intraventricular hemorrhage. *J Neuroinflamm 2019; 16:122.*

III. **Romantsik O**, Bruschettini M, Ley D. Intraventricular hemorrhage and white matter injury in preclinical and clinical studies. *NeoReviews 2019; 20:e636-e652.*

IV. **Romantsik O**, Erlöv T, Russo C, Meirza B, Gottschalk M, Cinthio M, Ley D. High-frequency ultrasound compared to magnetic resonance imaging for the volumetric reconstruction of ventricular size following cerebral intraventricular hemorrhage in the preterm rabbit. *Submitted to Ultrasonography.*

V. **Romantsik O**, Ross-Munro E, Grönlund S, Holmqvist B, Brinte A, Gerdtsson E, Vallius-Kvist S, Bruschettini M, Wang X, Fleiss B, Ley D. Post-hemorrhagic ventricular dilatation following IVH in the preterm rabbit pup: neurological function and cortical development. *In manuscript.*

Papers not included

Smeds E, **Romantsik O**, Jungner Å, Erlandsson L, Gram M. Pathophysiology of extracellular hemoglobin: use of animal models to translate molecular mechanisms into clinical significance. *ISBT Science Series 2017; 12:134-141.*

Agyemang AA, Sveindóttir K, Vallius S, Sveindóttir S, Bruschettini M, **Romantsik O**, Hellström A, Smith LEH, Ohlsson L, Holmquist B, Gram M, Ley D. Cerebellar exposure to cell-free hemoglobin following preterm intraventricular hemorrhage: Causal in cerebellar damage? *Transl Stroke Res 2017; 8:41.*

Jungner Å, Vallius S, Bruschettini M, **Romantsik O**, Gram M, Ley D. Cardiopulmonary bypass in the newborn: effects of circulatory cell-free hemoglobin and hyperoxia evaluated in a novel rat pup model. *Intensive Care Med Exp 2017; 5:45.*

Gumus HG, Agyemang AA, **Romantsik O**, Sandgren R, Karlsson R, Gram M, Vallius S, Ley D, Van den Hove DLA, Bruschettini M. Behavioural testing and litter effects in rabbits. *Behav Brain Res 2018; 353:236-241.*

Jungner Å, Vallius Kvist S, **Romantsik O**, Bruschettini M, Ekström C, Bendix I, Herz J, Felderhoff-Mueser U, Bibic A, In Apos T Zandt R, Gram M, Ley D. White Matter Brain Development After Exposure to Circulating Cell-Free Hemoglobin and Hyperoxia in a Rat Pup Model. *Dev Neurosci 2019; 41:234-246.*

Abbreviations

A1M, alpha-1-microglobulin

AQP1, aquaporin 1

BBB, blood-brain barrier

CPE, choroid plexus epithelium

CSF, cerebrospinal fluid

CTIP, chicken ovalbumin upstream promoter transcription factor interacting protein

GA, gestational age

GFAP, glial fibrillary acidic protein

GM, gray matter

Hb, hemoglobin

HFU, high-frequency ultrasound

HE, hematoxylin eosin

IF, immunofluorescence

IGF-1, insulin-like growth factor 1

IHC, immunohistochemistry

IL, interleukin

IVH, intraventricular hemorrhage

MBP, myelin basic protein

MMP, matrix metalloproteinase

MRI, magnetic resonance imaging

NECAB, neuronal Ca^{2+} binding protein

NeuN, neuronal nuclear antigen

NICU, neonatal intensive care unit

OF, open field

ORT, object recognition task

PAR, protease-activated receptor

PBS, phosphate buffer saline

PFA, paraformaldehyde

PHVD, post-hemorrhagic ventricular dilatation

PO, peroxidase activity

PND, postnatal day

PNN, perineuronal network

PreOLs, preoligodendrocytes

PSA-NCAM, polysialic acid neural cell adhesion molecule

PT, preterm

PV, parvalbumin

RBCs, red blood cells

ROI, regions of interest

ROS, reactive oxygen species

SEM, scanning electron microscopy

SFO, subfornicular organ

SPAK, Ste20-type stress kinase

TEM, transmission electron microscopy

TGF-β, transforming growth factor beta

TLR, toll-like receptor

TNF-α, tumor necrosis factor alpha

VEGF, vascular endothelial growth factor

WM, white matter

Preface

The survival of extremely preterm infants, especially those born below gestational age 26 weeks, has increased over the past decade due to tremendous improvement of perinatal care. However, the rate of major co-morbidities of extremely premature birth, in particular, that of intraventricular hemorrhage (IVH), remains constant. Nearly one-third of premature infants are affected by some degree of IVH, the proportion is even higher (up to 45%) in infants born below gestational age 26 weeks. Preterm infants with severe IVH have a high risk for the development of post-hemorrhagic ventricular dilatation (PHVD).

Intraventricular hemorrhage and PHVD are associated with a wide range of long-term neurodevelopmental impairment and behavioral deficits, leading to special educational needs. Despite nearly one hundred years of research in the field of IVH disease, there is still no treatment available. Thus, furthered understanding of pathophysiological mechanisms leading to complex brain damage is essential to discover and develop treatment strategies.

It is believed that extravasation of blood products following IVH plays a crucial role in further brain damage. Here, we highlight the role of extracellular Hb in the pathogenesis of secondary brain injury following IVH. Furthermore, we describe a novel model of PHVD in preterm animals and characterize the long-term effects of IVH on white and gray matter injury and the disruption of normal corticogenesis.

Abstract

Intraventricular hemorrhage (IVH) is one of the major co-morbidities of premature birth and is associated with post-hemorrhagic ventricular dilatation (PHVD), long-term neurodevelopmental impairment, behavioral problems, special educational needs, and dependency on health services.

Hypothesis and aims: We proposed that extravasated blood with release of extracellular hemoglobin (Hb) are crucial in brain injury following IVH and of consequent development of PHVD. The overall goal of this project focused on furthering pathogenetic insights of WM and GM injury following IVH and the development of possible neuroprotective treatment strategies that may promote brain development in preterm infants.

Methods: *Paper I.* We characterized extracellular Hb distribution within preriventricular WM in preterm rabbit pups following IVH. *Paper II.* We evaluated the cerebral biodistribution and possible functional neuroprotection of intracerebroventricularly (*i.c.v.*) administered alpha-1-microglobulin (A1M), a heme and free radical scavenger, in preterm rabbit pups following IVH. *Paper III.* We conducted a comprehensive review of preclinical and clinical studies on WM injury following IVH. *Paper IV.* We evaluated high-frequency ultrasound (HFU) as a tool for the reconstruction of volumetric volume in preterm rabbit pups with PHVD and compared its accuracy and reliability with that of a gold-standard – magnetic resonance imaging (MRI). *Paper V.* We established a novel model of PHVD in preterm rabbit pups and characterized the survival, neurobehavior, WM, and GM injury, as well as altered corticogenesis.

Results: *Paper I.* Extracellular Hb was widely distributed throughout the brain WM, in particular within periventricular WM with high extracellular plasticity following IVH. *Paper II.* Exogenous A1M (recombinant human) was extensively distributed within brain WM with further protraction into cerebellar WM following IVH. Moreover, it exhibited high co-existence with extracellular Hb. Administration of A1M (A1M derived from human plasma) decreased pro-inflammatory and oxidative damage. *Paper III.* A wide range of animal models have been used to explore pathogenetic mechanisms of IVH and related brain damage; possible targets enhancing brain damage have been identified. Nevertheless, the effectiveness of potential interventions is still limited. *Paper IV.* HFU-based volumetric reconstruction of brain ventricles is highly accurate and reliable as compared to MRI and may be a promising bed-side tool for evaluating of progression of PHVD in preterm infants. *Paper V.* IVH and PHVD lead to a long-term alteration of cortical myelination microstructure, disruption of cortical organization, selective reduction in neurogenesis and synaptogenesis, reduction in PV-positive interneurons.

Conclusions: Extracellular Hb travels easily through brain WM following IVH and it may be one of the key factors causal in furthered brain damage by triggering pro-inflammatory and oxidative cascades. Furthermore, IVH, leading to PHVD, disrupts normal corticogenesis, alters myelin microstructure, and causes a selective reduction in neurons, interneurons, and synapsis. A1M, as heme and free radical scavenger, attenuates WM damage, confirming that extracellular Hb is causative in ongoing neuroinflammation following IVH. Thus, A1M may be a possible treatment strategy in preterm infants with IVH. HFU represents an accurate tool for volumetric reconstruction of ventricles for diagnosis and management of PHVD.

Introduction

Intraventricular hemorrhage

Intraventricular hemorrhage (IVH), defined as bleeding within brain ventricles, is a serious co-morbidity of preterm (PT) birth. Its incidence remains constant despite extensive achievements in perinatal/ neonatal care (1,2). The stability in the incidence of IVH during the past two decades is related to improved survival of extremely PT infants (born below gestational age 28 weeks), particularly those born below gestational age 26 weeks (1–4). Extremely PT infants are highly vulnerable and approximately one-third of these newborns have some degree of IVH, with severe IVH (≥ grade III) occurring in nearly 30% of those infants (2,5,6). Nearly 60% of PT newborns diagnosed with severe IVH (≥ grade III) will develop post-hemorrhagic ventricular dilatation (PHVD) (2,7). The presence of IVH, independently of grade, increases the risk for adverse neurodevelopmental and behavioral outcomes; yet, infants with PHVD have a greater burden of significant motor and cognitive impairment (8–13), leading to special educational needs and a life-long dependency on social security. Currently, there is no effective treatment for IVH and thereby no means to prevent either development of PHVD or adverse neurodevelopmental/ behavioral outcome.

Pathophysiology of IVH

The pathogenesis of IVH disease in PT infants is very complex and still not entirely known. It is believed that bleeding arises in the germinal matrix and with further rupture of the ventricular ependyma it may progress into an IVH. The germinal matrix is a highly vascularized area, located between the ependymal lining of the lateral ventricle and the nucleus caudate. The germinal matrix has a high metabolic demand due to the presence of intensely dividing neuronal and glial progenitor cells that promote the normal development of the brain. It has been shown that the germinal matrix reaches its greatest thickness by GA 24 weeks with subsequent nearly complete involution by GA 36 weeks (14,15). The vasculature of the germinal matrix is highly fragile due to its unique characteristics, such as a high endothelial proliferative rate, expression of vascular endothelial growth factor (VEGF) and angiopoietin-2, deficient coverage of pericytes, and a lower expression

of transforming growth factor β (TGF-β) and fibronectin-1 (15), resulting in a propensity to bleed. In agreement with these findings, the incidence of germinal matrix hemorrhage may be decreased by prenatal administration of angiogenic inhibitors in the PT rabbit model (16). The other risk factors include rapid fluctuations in cerebral blood flow following PT delivery, hypoxia, hypercarbia, and coagulation abnormalities (17–19). Indeed, one of the strategies, shown to reduce the occurrence of IVH, is delayed umbilical cord clamping (20). It may be that by increasing the circulating blood volume through delayed umbilical cord clamping the stabilization of the cerebral blood flow is achieved. Furthermore, delayed umbilical cord clamping may have a stabilizing impact on the blood-brain barrier (BBB) by transfusing stem cells, growth factors, exosomes, microvesicles, anti-inflammatory substances, coagulation factors, platelets, and Hb scavengers.

IVH mainly occurs during the first week of life, particularly within the first 72h of life due to a major hemodynamic instability of the PT infant (5).

Diagnosis and grading of IVH

The diagnosis of IVH is usually done by brain ultrasound examination, which is routinely performed in all PT infants born below GA 32 weeks at postnatal days (PND) 1, 3, 7, and 14 (21); the frequency of further brain ultrasound examination is institution dependent. Brain ultrasound is also a reliable tool to follow PHVD development to support the decision-making on interventions aiming to alleviate intracranial pressure and ventricular dilatation.

There are two different classifications available for the grading of IVH – Papiles (22) and Volpe (23). The first three grades, from I to III, are similar in both classification systems and they are defined as follows: grade I: the hemorrhage is limited to the germinal matrix; grade II: the hemorrhage extends from the germinal matrix into the brain ventricles, occupying < 50% of the ventricular volume; grade III: a further extension of hemorrhage to more than 50% of ventricular volume resulting in ventricular dilatation. As for Papile, the definition of grade IV, based on interpreting intraventricular bleeding as a continuum, is intraventricular hemorrhage with a parenchymal extension (22). Volpe suggested using grade IV IVH as a separate entity, as it represents periventricular hemorrhagic venous infarction instead of IVH extension into the parenchyma (23). Indeed, periventricular hemorrhagic venous infarction may be associated with any grade of IVH (Figure 1).

Grade III and IV IVH are also frequently defined as severe hemorrhages with a higher risk for the adverse neurodevelopmental outcome (1,24,25).

18
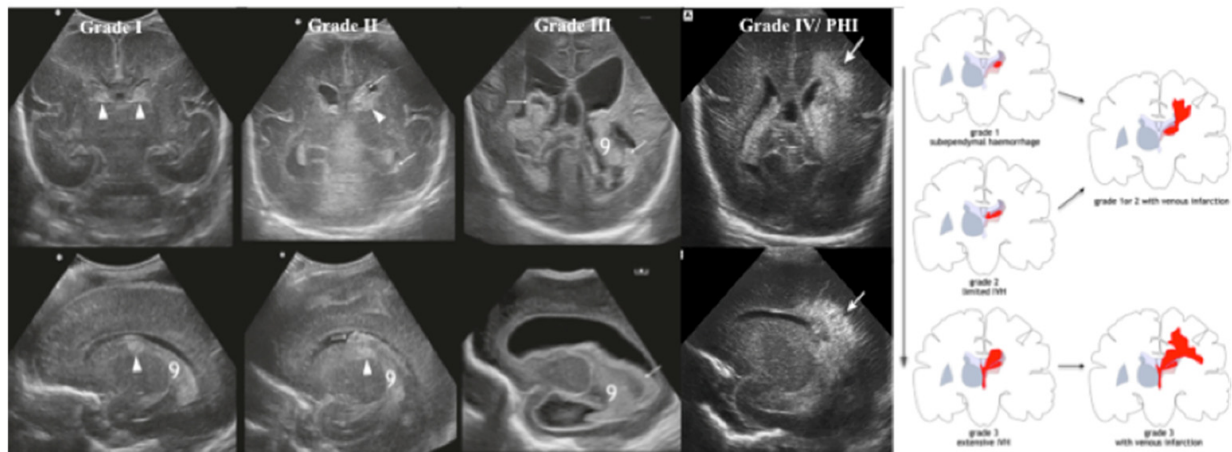
Figure 1. Ultrasound-based IVH grading. Reprinted from "Cranial ultrasound findings in preterm germinal matrix haemorrhage, sequelae and outcome", by Parodi A, Govaert P, Horsch S, Bravo CM, Ramenghi L on behalf of the eurUS.brain group. Pediatr Res 2020; 87:13-24. Copyright Springer Nature 2020 (26).

Post-hemorrhagic ventricular dilatation

It has been shown that nearly 60% of PT infants with severe IVH (≥ grade III) will develop PHVD (2,7); of those, 38-87% of infants will require ventriculo-peritoneal shunt placement which in turn is associated with secondary shunt-related complications (27).

The diagnosis of PHVD and the decision to intervene neurosurgically are based on two-dimensional (2D) ventricular size measurements: ventricular index (VI), the anterior horn width, and thalamo-occipital distance (TOD) (28,29) (Figure 2.) (30).
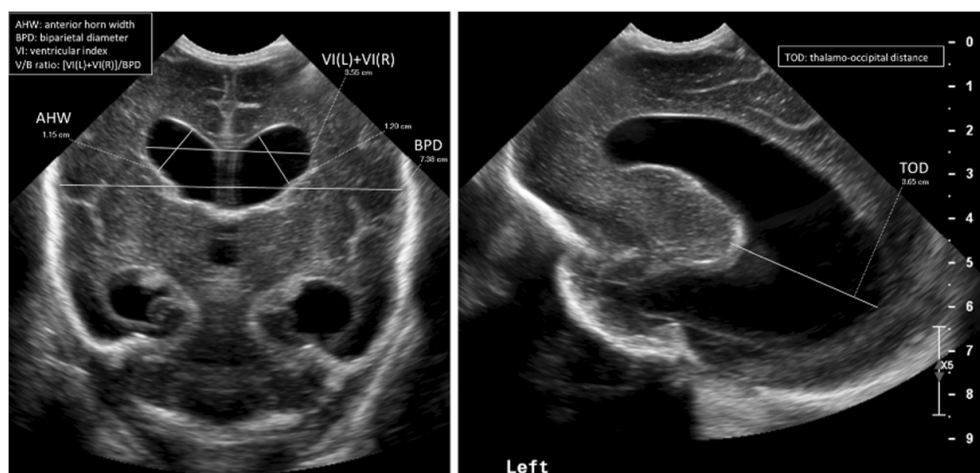
Figure 2. Ultrasound-based 2D measurements of ventricular size in a preterm infant with PHVD. Reprinted from "Preterm neuroimaging and neurodevelopmental outcome: a focus on intraventricular hemorrhage and posthemorrhagic hydrocephalus, and associated brain injury", by Dorner RA, Burton VJ, Allen MC, Robinson S, Soares BP. J Perinatol 2018; 38:1431-1443. Copyright Springer Nature 2018 (30).

IVH-induced brain injury

Despite the considerable amount of research focused on IVH, the molecular mechanisms responsible for brain injury are still not entirely understood. Brain injury following IVH may be divided into 2 different phases; the primary injury, when actual bleeding occurs, and the secondary injury, which is induced by neuroinflammation triggered by the presence of blood products.

Primary brain injury

There are at least three physical effects of IVH: displacement of neural tissue (mass effect), increased intracranial pressure, and the blockage of cerebrospinal fluid (CSF) pathways. Once the hematoma is formed, it generates mechanical pressure on the ventricular wall. It has been shown in the fact that infants with severe IVH and subsequent diagnosis of PHVD exhibit an early alteration in visual evoked potentials and amplitude-integrated electroencephalography, which normalize after successful CSF evacuation (31,32).

Furthermore, the hematoma may cause temporary obstruction of the CSF drainage pathway, either in the ventricular system or at the CSF outflow sites (33). It is believed that such obstruction may contribute to PHVD development due to the shift of CSF homeostasis. The blockage of CSF drainage due to blood clots and fibrosis results in decreased CSF reabsorption. On the other hand, it has been demonstrated elegantly that there is a hypersecretion of CSF following IVH (34). This seems to be dependent on activation of Toll-like receptor-4 (TLR) and a nuclear factor kB-dependent inflammatory response within choroid plexus epithelium (CPE) (34). This leads to Ste2o-type stress kinase activation (SPAK) that results in phosphorylation of Na/K/Cl co-transporter (NKCC) $_I$ at the apical surface of CPE (34) (Figure 3). These data were supported by models of genetic depletion of TLR4 or SPAK, in which CSF secretion was re-established and PHVD symptoms improved (34). Besides, inhibition of TLR4-nuclear factor-kB signaling or the SPAK-NKCC$_I$ complex diminishes CSF hypersecretion and by that also PHVD related symptoms (34).
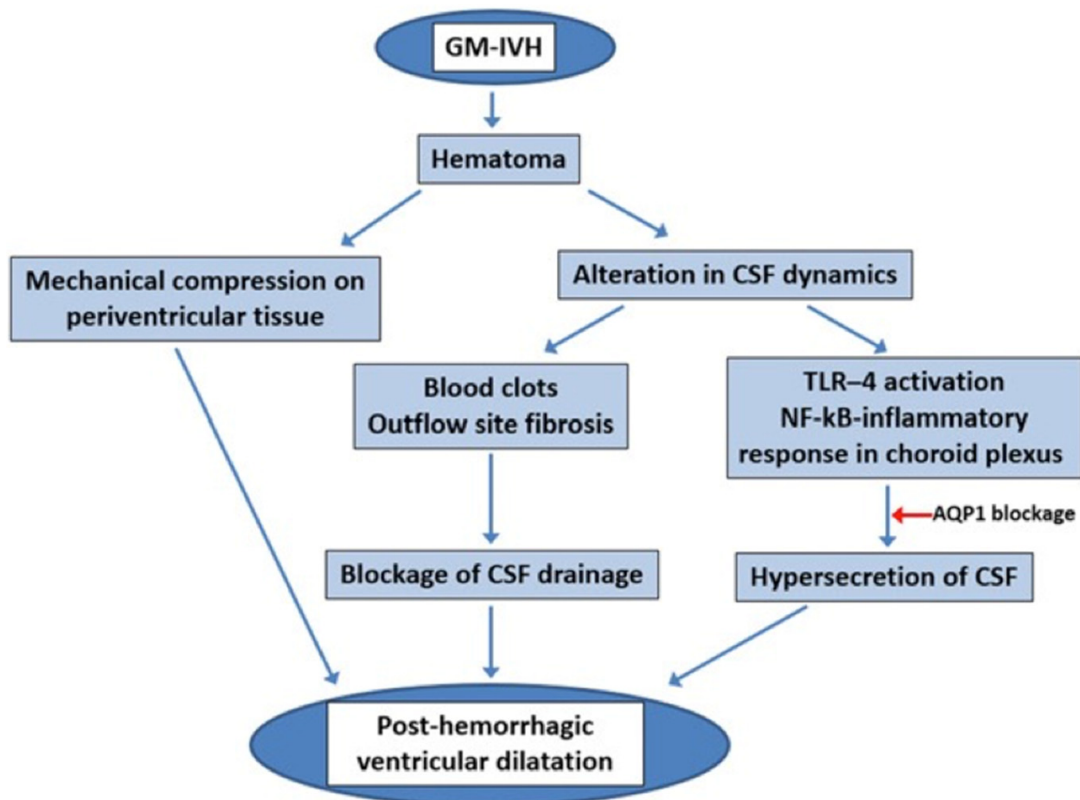
Figure 3. Primary brain injury following IVH: impact om hematoma mass effect. AQP1 = aquaporin 1, CSF = cerebrospinal fluid, NF-kB = nuclear factor-kB, TLR = Toll-like receptor. Reprinted from "Intraventricular hemorrhage and white matter injury in preclinical and clinical studies", by Romantsik O, Bruschettini M, Ley D. NeoReviews 2019; 20:e636-e652. Copyright American Academy of Pediatrics 2019 (35).

The CPE contains tight junctions between the cells on the ventricle-facing site and a broad spectrum of ion transporters and water channels. The CPE is involved in the active transport of sodium ions into the ventricles and water obeys the consequent osmotic gradient. Among the different water channels, aquaporin 1 (AQP1) is suggested to have a crucial role in transcellular water transport and normal homeostasis of CSF (36). Indeed, AQP1 knockout mice CPE is characterized by a reduced water permeability by 80% with a simultaneous decrease in CSF secretion rate by 35% (37). Additionally, AQP1 protein expression in CPE was enhanced following IVH in PT rabbit pup (38).

Clearing the hematoma following IVH may reduce the mass effect and by that the level of toxic blood products within the brain. In fact, the DRIFT (drainage, irrigation, and fibrinolytic therapy) study, despite the observed increase in secondary hemorrhages, showed that at 2 and 10 years of age there was an improvement of cognitive function and reduction in death or severe disability (12,39). These results open up new perspectives for possible PHVD treatment strategies, however, more efficacy and safety data are needed. It seems also that targeting TLR4 and AQP1 may present possible treatment strategies.

Secondary brain injury

It is believed that blood products play a central role in secondary brain injury following IVH. Since the onset of hemorrhage, a considerable amount of erythrocytes are hemolyzed with the release of extracellular Hb and its metabolites. Furthermore, platelets, immune cells, coagulation factors are also released and they may contribute independently to further brain damage (Figure 4).

Coagulation factors

Indeed, thrombin production, which is essential to prevent bleeding by converting soluble fibrinogen into insoluble fibrin, is promptly increased (40) and in low concentration, it has a neuroprotective role (41,42). Nevertheless, at high concentration thrombin may be detrimental for brain tissue (40) due to its involvement in brain edema formation and ischemic injury (43), neuronal and astrocyte death (43,44). Thrombin acts through the protease-activated receptor (PAR) I, PAR-3, and PAR-4 (45,46). Of note, PAR-I activation following IVH results in CPE damage and activation of metalloproteinases (MMP), particularly MMP9, which results in further disruption of BBB, induces apoptosis, and supports the development of PHVD (47,48). Several studies have shown that inhibition of PAR-I, Src family kinases, and/or MMP 9/ MMP 2 attenuate brain edema development and infiltration of inflammatory cells (48,49).

Another coagulation factor – fibrinogen – seems to be also involved in secondary brain damage. Extravasated fibrinogen triggers an inflammatory response through activation of microglia CD_{IIb}/CD_{18} receptor and aggravates brain injury (50).

Platelets

Following the bleeding extravasation of platelets occurs and transforming growth factor β (TGF- β) is released. TGF- β leads to fibrosis formation and obstruction of CSF outflow sites (51). It has been demonstrated that a TGF-β antagonist, decorin, can attenuate ventriculomegaly and WM injury (52,53). Additionally, activated platelets release lysophosphatidic acid that may support the disintegration of ependymal integrity (54,55).
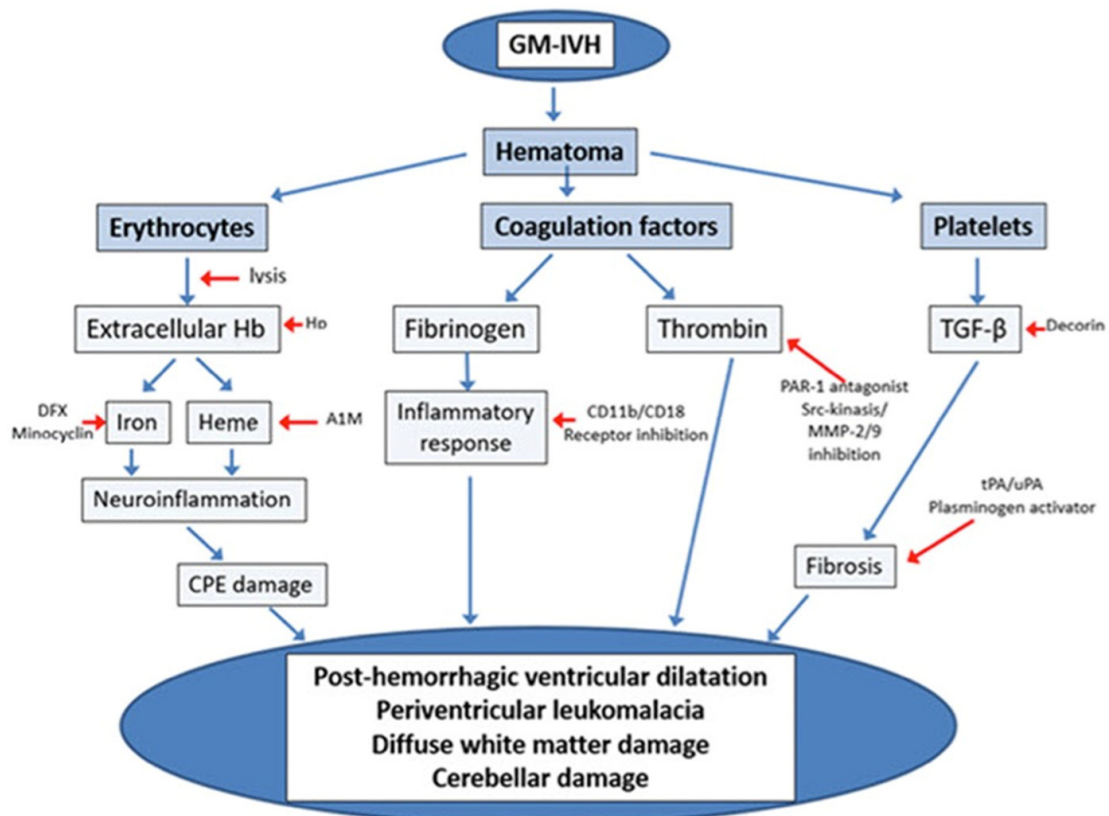
Figure 4. Pathological mechanisms underlying the formation of PHVD, periventricular leukomalacia, diffuse WM injury, and cerebellar damage. A1M = alfa-1-microglobulin, CPE = choroid plexus epithelium, DFX = deferoxamine, Hb = hemoglobin, Hp = haptoglobin, MM= = matrix, metalloproteinase, PAR = protease-activated receptor, TGF-β = transforming growth factor β, tPA/uPA = tissue and urokinase plasminogen activator. Reprinted from "Intraventricular hemorrhage and white matter injury in preclinical and clinical studies", by Romantsik O, Bruschettini M, Ley D. NeoReviews 2019; 20:e636-e652. Copyright American Academy of Pediatrics 2019 (35).

Extracellular hemoglobin (Hb) and its degradation products

Extravasation of blood into the ventricles leads to hemolysis with a discharge of extracellular Hb into CSF (56). Extracellular Hb is very reactive, and setting off the cytotoxic, oxidative, and inflammatory pathways, induces tissue damage (57,58). Extracellular Hb becomes redox-active, which results in the formation of ferric Hb (Fe^{3+}), also known as MetHb, and the release of the heme group (56,59) (Figure 5 A). Free heme accelerates the generation of reactive oxygen species (ROS) and is a source of redox-active iron that through its participation in Fenton's reaction produces toxic hydroxyl radicals, which amplifies the production of ROS (60). This causes not only damage to cell membranes and cell membrane-bound proteins, but also damage to mitochondria and DNA (60) (Figure 5 B). Furthermore, it has been shown that free heme oxidizes low-density lipoproteins and depletes nitric oxide, thus inducing endothelial dysfunction (61).
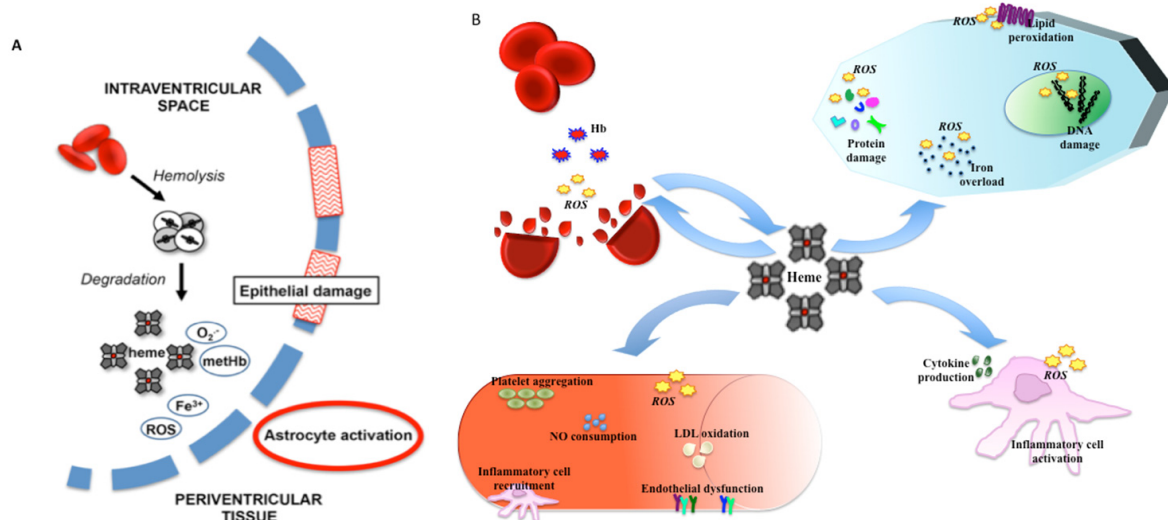
Figure 5. A. Degradation of Hb following IVH. Extravasated erythrocytes undergo lysis with a rapid release of Hb with the formation of MetHb and further degradation resulting in the release of heme, free iron, and free radicals. Reprinted from "Pathological conditions involving extracellular Hb: molecular mechanisms, clinical significance and novel therapeutic opportunities for a1-microglobulin", by Olsson MG, Allhorn M, Bulow L, Hanson SR, Ley D, Olsson ML *et al.* Antioxidants and Redox signaling 2012; 5:813-846. Copyright Mary Ann Liebert 2012 (58). **B. Heme toxicity.** Following the lysis of erythrocytes, extracellular Hb is released and undergoes degradation with the release of heme. Free heme is known to be hemolytic and supports further rupture of erythrocytes. Heme induces cellular oxidative damage through the formation of ROS, lipid peroxidation, amplifying the production of ROS which leads to protein damage, mitochondrial damage, and DNA fragmentation. Free heme is a strong pro-inflammatory trigger - it activates cytokine production and inflammatory cell activation. Moreover, heme causes endothelial dysfunction by oxidative consumption of NO, recruitment of inflammatory cells, activation of adhesion molecule expression and favoring platelet aggregation, oxidation of low-density proteins (LDL).

The structural damage to the CPE caused by extracellular Hb has been observed as soon as 24 hours IVH, followed by cellular decomposition, characterized by loss of normal villous morphology and cellular death signs 72 hours later in the PT rabbit pup IVH model (56,62). Additionally, metHb concentration seems to be correlated to an elevation of pro-inflammatory cytokine – tumor necrosis factor-alpha (TNF-α) - in the CSF of the PT rabbit pup and PT human infants (56,62). TNF-α is a powerful inducer of inflammation, leading to pre-oligodendrocyte (PreOL) apoptosis (63) and arrest of the normal branching of neurons (64).

The release of free iron results in the accumulation of the non-protein bound iron and ferritin along the ependymal lining, leading to long-lasting up-regulation of cerebral ferritin (65,66). Of note, free iron was also found in CSF of PT human infants with PHVD (67). The presence of free iron in the ependymal lining provokes damage, leading to the formation of denudation areas and promotes extracellular Hb movement into periventricular WM. Indeed, as a part of this thesis project, we demonstrated the penetration and wide distribution of extracellular Hb within periventricular WM. This finding is of extreme importance because periventricular WM is rich in PreOLs, which progressively differentiate to mature oligodendrocytes (OLs). The peak activity for this process happens to be between GA 23-35 weeks (68,69). PreOLs are highly sensitive to oxidative stress, inflammation, and hypoxic-

ischemic episodes (68,69). The damage to PreOLs is one of the key factors for WM injury in PT infants and it is characterized not only by the arrest of PreOL maturation and hypomyelination but also by alteration of myelin microstructure (70–72).

After extracellular Hb is released into the CSF following IVH, extracellular Hb and its metabolites are deposited on the cerebellar surface, causing altered cerebellar cortical development, dysmaturation of Purkinje cells, and deficient proliferation of neuronal progenitors (73–75).

IVH and cortical development

The release of blood products into the ventricular space following IVH triggers the activation of an inflammatory cascade, characterized by microglia and astrocyte activation, immune cell infiltration, death of neural and glial cells, the inhibition of PreOL maturation, and hypomyelination. The inflammation may last for several weeks (76) leading not only to a well-described diffuse WM injury but affecting brain GM as well. Recent clinical studies in PT human infants demonstrated a reduced cortical and subcortical GM volume (77,78). The reductions in the volume of the nucleus caudate, cortex, and hippocampus were associated with adverse neurocognitive outcomes and behavioral disorders (72,77,79,80). Apart from the volume reduction of brain GM, an aberrant architecture of the cerebral cortex has been reported (81). Indeed, Dieni *et al.* observed areas of neuronal necrosis in deep cortical layers (layers V-VI) and in nucleus caudate (82). Moreover, in human post-mortem studies, it has been demonstrated that interneurons are particularly vulnerable to perinatal brain injury (83,84). Similar data were reported in a sheep model of fetal hypoxia-ischemia with specific loss of interneurons and their perineural networks (PPN) in the cortex as well as a simplified arborization and spine density in the cortex hippocampus and caudate nucleus (85–87).

This wide spectrum of injury patterns, involving both WM and GM may lead to disruption of connectivity, leading to remodeling of cortical circuits, and potentially to the adverse neurodevelopmental outcome and behavioral problems.

Parvalbumin (PV) positive interneurons

As mentioned above, cortical interneurons, in particular PV-positive interneurons, seem to be vulnerable to damage as they migrate and mature at the time of PT delivery (84,88). PV-positive interneurons are GABAergic interneurons that bind Ca^{2+} and reduce pre-synaptic Ca^{2+} concentrations thereby supporting short-term synaptic plasticity (89). Moreover, they have a fast-spiking action potential which in turn requires a high metabolic rate (89). In the cortex, PV positive interneurons

form networks via electrical and chemical synapses necessary for plasticity throughout life starting from birth (89). These networks are needed to create and maintain gamma oscillation, involved in the working memory. Panda *et al.* demonstrated the reduction of PV-positive interneurons in deep cortical layers in PT human infants (83). A very recent study in two rodent models of encephalopathy of prematurity demonstrated a reduction of PV positive interneurons in the cortex and hippocampus (90).

Perineural networks (PNN)

Perineural networks (PNN) represent a kind of extracellular matrix, that embeds the soma and proximal dendrites of several types of neurons, particularly GABAergic neurons, including PV positive interneurons (91). PNNs are expressed in the cortex, hippocampus, hypothalamus, amygdala, and cerebellum (91). The expression of PNN appears to be regulated by the homeobox protein orthodenticle homeobox-2 (Otx2) (92). Intriguingly, Otx2 is believed to be released by the choroid plexus and taken up by PV-positive cells during their normal process of maturation (93,94). Tight regulation of PNNs is required for normal neural connectivity (91,95) (Figure 6). In fact, the population of PV positive interneurons with PNNs is decreased in hypoxic-ischemic and inflammatory brain injury (84,87).
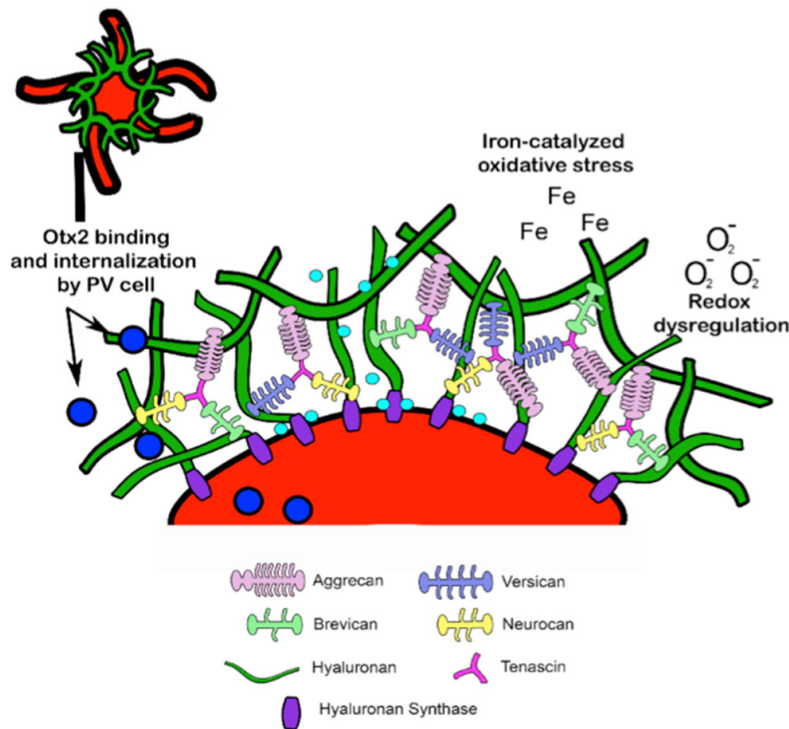
Figure 6. Structural composition of PNN. PNN is composed of a linear hyaluronic acid polymer that forms the foundation of the structure. Aggrecan, versican, brevican, neurocan (belong to chondroitin sulfate proteoglycans (CSPGs)) are connected to a hyaluronic acid polymer by link proteins such as cartilage link protein 1. Tenascin is joined to the C-terminal domains of CSPG to complete the structure. PV positive interneurons embedded with PNN are safeguarded from redox activity and oxidative stress such as free iron or free radicals. Furthermore, PNNs are involved in PV positive interneurons maturation process through internalization with Otx2 homeobox proteins (released from choroid plexus). Reprinted from "The perineural "safety" net? Perineural net abnormalities in neurological disorders", by Wen TH, Binder DK, Ethel IM, Razak KA. Frontiers Mol Neurosci 2018;11:270. Copyright Frontiers Media SA 2018 (96).

Based on the above, we focused as part of this thesis on investigating the PV positive interneuron population and its association with PNN in PT rabbit pups following IVH with established PHVD.

Neutralization of extracellular Hb

Available data indicate that extracellular Hb and its metabolites may be central in secondary brain injury following IVH. Therefore, neutralizing extracellular Hb and its metabolites may constitute a potentially valuable treatment strategy. There are several endogenous systems involved in the scavenging of extracellular Hb, such as haptoglobin (Hp), hemopexin, albumin, high- and low-density lipoproteins, and alpha -1-microglobulin (A1M) (58) (Figure 7).
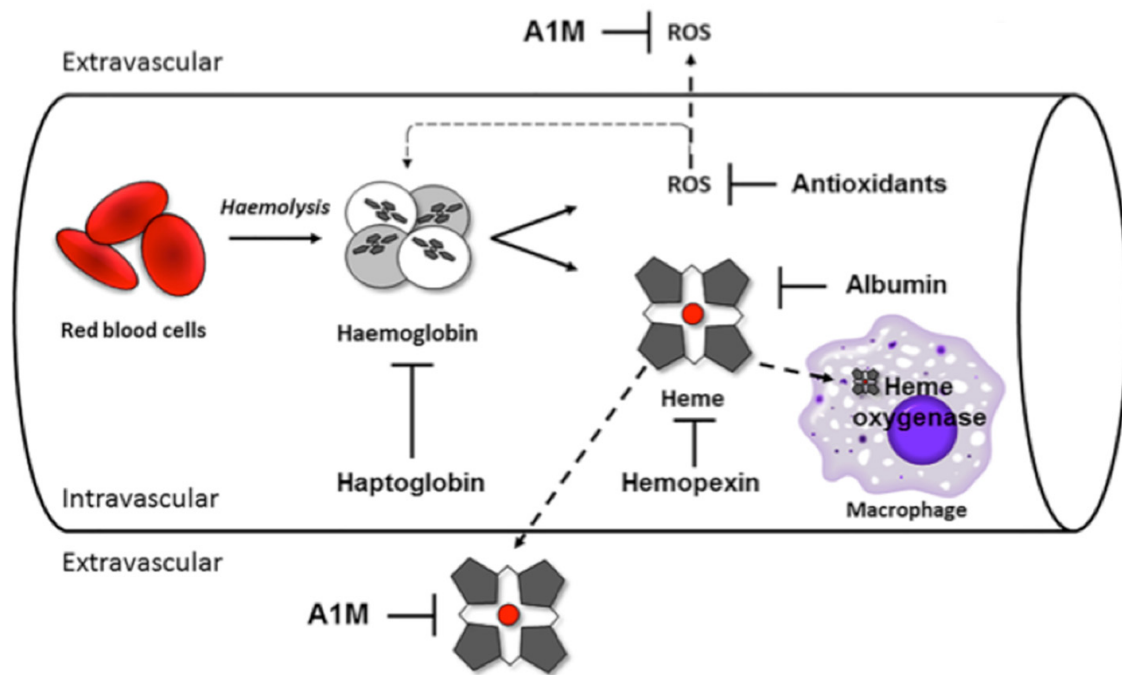
Figure 7. Endogeneous systems involved in the neutralization of extracellular Hb and its metabolites. Haptoglobin (Hp) binds intravascular extracellular Hb forming a stable Hp-Hb complex, which undergoes intracellular endocytosis. Free heme is captured by hemopexin and degraded by heme oxygenase intravascularly, whereas extravascularly heme and free radicals are sequestered by alpha-1-microglobulin (A1M) with subsequent renal elimination. Reprinted from "Pathophysiology of extracellular haemoglobin: use of animal models to translate molecular mechanisms into clinical significance", by Smeds E, Romantsik O, Jungner Å, Erlandsson L, Gram M. VOXS 2017; 12:134-141. Copyright John Wiley and Sons 2016 (97).

A1M is a potent tissue-protective protein acting through free heme binding, free radical scavenging, reductase activity, and its ability to bind to mitochondria (58,98,99). While binding to mitochondria during the early stages of cell death A1M can attenuate heme- and ROS-induced mitochondrial swelling (100). Interestingly, the brain has its production of A1M, displayed in the minute quantity in CSF in comparison to other body fluids (101). Furthermore, in adult patients with intracranial hemorrhage an increase in endogenous A1M concentration in CSF has been reported (102). However, it is still unknown whether local cerebral production of A1M is increased or the rise in concentration is related to BBB disruption (102).

Recently, a recombinant human A1M (rA1M) has been developed, which seems to be functionally equivalent to A1M obtained from human plasma (hA1M) (103,104). Thus, A1M seems to be a potential therapeutic agent based on its properties and established characteristics of IVH pathogenesis, which in turn may be beneficial for future neurodevelopmental outcome in PT infants with IVH.

Preterm rabbit pup IVH model

The disease of IVH is extremely complex similar to a 5000 piece subtle color gradient puzzle. Based on that, a broad spectrum of different animal models of IVH has been applied, including mice, rats, rabbits, cats, dogs, piglets, and even primates (17–19,82,105–114). The animals in most of those models are born at term with mature systemic physiology in conjunction to a diverse degree of cerebral maturity varying from PT (rodents) to term (piglets, cats, dogs) as compared to the human infant (115). If actual PT birth is not present in the model several important features of prematurity will be omitted such as respiratory instability, the deficit of trophic factors, deficiency of coagulation system, and the hemorrhage impact in immature brain tissue.

Although no animal model can entirely resemble the human PT circumstances, the PT rabbit IVH model may be one of the more pertinent small translational animal models of IVH. The delivery of PT rabbit pups through cesarean section occurs at postconceptional day 29 (full-term = 32 days) and at this point rabbit pups exhibit many similarities in their systemic physiology to the human PT infant such as rudimentary alveolar structure (116), tendency to develop NEC–similar disease (117), renal immaturity (118) and trophic factor such as IGF-1 deficiency (119). The brain development at the postconceptional day in PT rabbit pups corresponds to circa GA 24-25 weeks in human infants (113,120). Of note, up to 10% of PT rabbit pups bleed spontaneously into the ventricles (121,122). Unlike rodents, rabbits are "perinatal brain developers", having the brain growth velocity spurt immediately prenatally and postnatally during the first month of life (123). The brain structure of the rabbit is more complex compared to rodents with a higher proportion of WM (124,125). Additionally, dissimilar to rodents and piglets, whose corticospinal tract myelination is more advanced at the time of the IVH insult (PND 7 in rodents and approximately 9-22h of age in term piglets) (115) rabbits´ myelination process starts at postnatal day (PND) 4 and reaches its peak around PND 18 (113,126).

Unlike the rodent and piglet IVH model, where IVH is induced either by *i.c.v.* injection of centrifuged blood with high hematocrit concentration (105–109) or by injection of collagenase (110,111,127), IVH in the PT rabbit pup is induced by intraperitoneal (*i.p.*) injection of glycerol. This prompts dehydration and a rise in serum osmolarity, followed by intracranial hypotension and a subsequent increase in the transmural pressure gradient over the vessel wall, resulting in the breach of the vessels within the germinal matrix (113,120,122). Such a mechanism is believed to mimic more closely the clinical situation of IVH in PT infants.

Wet-nurse

During the past three years we worked on improving and optimizing our PT rabbit pup model, which has resulted in the introduction of a wet-nurse (= a rabbit doe). The rabbit wet-nurse has been successfully used in intrauterine growth restriction studies (128). A wet-nurse gives birth vaginally to her pups at term within 24 hours of the planned PT delivery of another time-mated doe. On the day of cesarean section, all of her term pups, but two, are replaced with PT pups. The wet-nurse then takes care of and nurses all pups until the end of the study. Unlike common belief rabbit does are very good mothers. PT rabbit pups receive their first feeding through a feeding tube and after that, they are transferred to the wet nurse. By doing so we can reduce mechanical trauma to the digestive system (no insertion of a feeding tube) and hypothermia. The main advantage of using a wet-nurse is that pups are breast-fed and thus receive the beneficial effect of rabbit breast milk. Indeed, the beneficial effect of breastfeeding in PT rabbit pups was elegantly demonstrated by Klebe *et al.* (129). There is strong orocephalic stimulation and grasping movements while nursing due to the presence of a mammary pheromone in lactating does milk (130). Of note, mammary pheromone helps to establish a circadian rhythm in rabbits (131) and it is involved in odor processing and osmoregulatory circuits (132,133). The introduction of the wet-nurse has proved an enormous improvement to the model, because lactating does stimulate pup breathing, provide thermal control, attenuate the stress response, and by attention and directional stimulation support the pups learning and social behavior (134).

High-frequency ultrasound (HFU)

HFU (40MHz) has been proven to be a reliable and accurate device for the diagnosis of IVH and monitoring of PHVD development in our PT rabbit IVH model (114). The spatial resolution of HFU is excellent, being as low as 40 μm in our setup. On the other hand, the penetration depth is limited to approximately 11mm, which is sufficient for the PT rabbit brain, but not for the PT infant brain (135). The major advantage of HFU is that it can be done by the animal-side without any sedation.
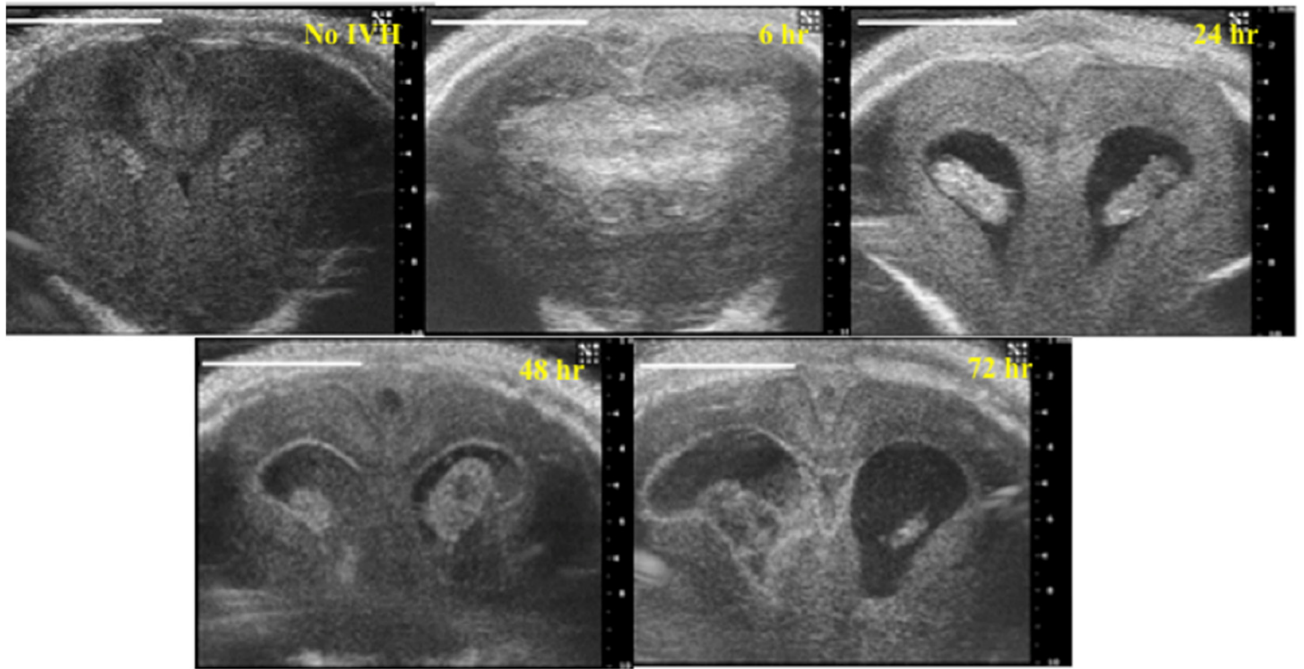
Figure 8. Diagnosis of IVH by HFU. The hemorrhage appears already at 6 hours after induction of IVH by *i.p.* injection of glycerol. IVH develops further into PHVD over 72 hours. Reprinted from " High-Frequency Ultrasound in the Evaluation of Cerebral Intraventricular Haemorrhage in Preterm Rabbit Pups", by Sveinsdottir S, Cinthio M, Ley D. Ultrasound in Med Biol 2012; 38: 423-431. Copyright Elsevier 2012 (114).

Hypothesis and aims

The basis for this thesis is the disease of IVH, which continues to be a serious problem worldwide, due to still lacking pieces in the pathological and molecular mechanisms leading to secondary brain damage and adverse neurodevelopmental outcome. This creates an immense challenge for the development of treatment strategies.

We believe that extracellular Hb and its metabolites are central in secondary brain damage following IVH by inducing long-lasting inflammation and oxidative stress. We hypothesize that PHVD results not only in WM damage but also affects cortical development and structure. We propose that treatment with a free heme scavenger may potentially prevent further brain injury following IVH and represent a possible treatment strategy for PT infants.

Paper I

Hypothesis
After IVH, there is a rupture of ventricular ependymal lining, and a considerable amount of RBCs and released extracellular Hb, i.e. not contained in the RBCs, penetrates over the barrier into the periventricular brain tissue.

Aim
To investigate the extent of penetration of extracellular Hb into periventricular WM following IVH in the preterm rabbit pup.

Paper II

Hypothesis
Administration of A1M, a heme and radical scavenger, may protect from secondary brain damage following IVH in the preterm rabbit pup.

Aim
To characterize the biodistribution of exogenous A1M within periventricular WM and to evaluate its protective effect in preterm rabbit pups with IVH.

Paper III

Hypothesis

A comprehensive review on IVH and its related WM injury in preclinical and clinical studies might help to identify research gaps and the effects of different types of interventions.

Aim

To review preclinical and clinical studies on IVH-related brain damage mechanisms and possible treatment strategies for preterm infants.

Paper IV

Hypothesis

High-frequency ultrasound may be a reliable tool for the reconstruction of ventricular volume in PHVD in preterm rabbit pup.

Aim

To evaluate HFU as a tool for reconstruction of ventricular volume in PHVD in the preterm rabbit pup IVH model.

To compare HFU accuracy and reliability with that of a gold standard – MRI – in the preterm rabbit pup IVH model.

Paper V

Hypothesis

There are little data available on long-term outcomes of IVH/PHVD in animal models, limited to term-born animals. The establishment and characterization of long-term follow-up of the IVH/PHVD model in preterm animals may help to fill the knowledge gap.

Aim

To establish a long-term IVH/PHVD model in the preterm rabbit pup.

To introduce a wet-nurse in the preterm rabbit pup IVH model.

To evaluate neurobehavioral assessment in the long-term IVH/PHVD preterm rabbit pup model.

To investigate WM and GM injury and cortical development in the long-term IVH/PHVD preterm rabbit pup model.

Methods and materials

Preterm animals

IVH preterm rabbit pup model

Paper I, Paper II, Paper IV, and Paper V

All conducted studies in this thesis were approved by the Swedish Animal Ethics committee in Lund (drn. M 2-16). We used the PT rabbit pup model of glycerol-induced IVH as previously described. The experiments were performed on PT rabbit pups born on postconceptional day 29 (term = 32 days). A half-breed between New Zealand White and Lop was used (Christer Månsson, Löberöd, Sweden). The pups were delivered prematurely by cesarean section after the does were anesthetized with i.v. propofol (5mg/kg, Primen Pharmaceuticals Oy, Helsinki, Finland).

This small animal model of IVH was chosen for all the studies, because it has several analogies with human PT birth, starting with similarities in placental development (136), immaturity of organ systems (116–119), the propensity to spontaneous IVH (121,122) and similarities of IVH development (113,114,120,122). Limitations of the model include a restricted control of the size and distribution of the glycerol-induced bleeding and overall reported mortality that varies from 40% to 70% (113,120,137).

Conditions, handling and protocols

following delivery, the pups were dried and rubbed to stimulate breathing, placed into an incubator, where they were marked for identification, weighed and handfed using a 3.5 French feeding tube (Vygon, Ecouven, France). The conditions, handling and protocols were different for the respective studies:

Nest, temperature and humidity

Paper I: The temperature was set at 34-35°C with ambient humidity throughout the study.

Papers II, IV: Temperature was set at 32°C with ambient humidity throughout the study. Moreover, we created a nest with rabbit doe fur and hay to make pups feel more comfortable and reduce stress.

Paper V: Temperature was set at 32°C with ambient humidity for a few hours after delivery until they were randomized (www.random.org) to a wet-nurse who was handled at ambient room temperature and humidity.

Feeding

Paper I: The PT pups were handfed with 2ml (100ml/kg/day) of kitten milk formula (KMR, PetAg Inc., Hampshire, IL, USA) with the first feeding done at circa 1-2h of age, subsequently every 12h, incrementing the milk volume by 1ml every 24h.

Papers II and IV: The onset of the feeding was similar to paper I, however, the amount of milk was subsequently increased every 24h by 25ml/kg/day.

Paper V: The pups were handfed just once at approximately 1 h of age with 100ml/kg of bovine colostrum (Whole Colostrum, ColoDan, Denmark). A few hours later, following randomization, PT rabbit pups were transferred to wet-nurse to be cared for by her throughout the whole experiment.

The pups handling conditions, including temperature, humidity, nesting, and feeding were modified over the years of the present PhD project as we were gaining more knowledge regarding the general care of PT rabbit pups. Several additional small studies were performed to assess the optimal milk composition, feeding frequency, and administered feeding volumes. Moreover, by observation of rabbit mothers, we learned to build the nest to attenuate the stress. Ultimately, we introduced a wet-nurse and we have learned that rabbits are excellent mothers with all the resulting benefits for the pups as described in the background section.

Postnatal growth

Paper I, II and IV: PT pups were weighed at birth and thereafter every 24 hours until the study end-point.

Paper V: All pups were weighed daily for 7 days, at PND 11, and after that every 6 days. Moreover, a bi-parietal measurement was performed at the same time-points.

The consistent finding across all the studies was a weight loss of up to 12% during the first 2 days of life, being stable or with 2-3% gain on the third day of life.

IVH induction

Paper I, II, IV and V: To induce IVH, the PT rabbit pups received *i.p.* injection of 50% (v/v) sterile glycerol (6.5g/kg; Teknova, Hollister, CA, USA) at 2-3h of age.

The rationale to induce IVH with an intraperitoneal injection of glycerol is the similarities with human PT infants regarding the onset of the hemorrhage and its pathophysiological appearance (113,114,122). When compared to the animal models of IVH, where centrifugated blood with elevated hematocrit is injected *i.c.v.,* germinal matrix vasculature remains intact and small periventricular infarctions, as

observed in PT rabbits and human PT infants, do not occur (113). While in the collagenase model of IVH, where the rupture of the vessels within the germinal matrix occurs with subsequent bleeding to the ventricles, it induces a notable inflammatory response (127). Moreover, in both models, there is a risk for a secondary brain injury due to a needle insertion through the brain parenchyma. Intraperitoneal glycerol injection results in systemic uptake of glycerol and may induce organ toxicity. This is one of the reasons why all of the PT rabbit pups included in our study receive glycerol injection.

Survival

Paper I: Results from 47 PT rabbit pups from 13 litters were presented in the study. The overall survival rate was 70%.

Papers II and IV: Results from 29 PT rabbit pups (females = 27) from 18 litters were presented in the study. The overall survival rate was 20%.

Paper V: Results from 21 PT rabbit pups (females = 4) from 12 different litters were presented in the study. The overall survival rate was 27%.

The scarce data are available on PT rabbit pups` survival which may vary from 40-70% within the first two weeks of life (113,120,137). It is difficult to explain the high rate of mortality in studies I and II, because the settings of the study were similar to the previous studies. Moreover, the pups from 2 litters died shortly after birth but before glycerol administration. The survival of control pups at PND 30 was 40% in paper V and in the study by van der Veeken *et al.,* the survival of PT rabbit pups in absence of any insult at PND 30 was 56% (138).

HFU for the detection of IVH

Paper I and II

Brain HFU (Visualsonic Vevo 2100, Visualsonics Inc, ON, Canada), using an MS-550D 40 MHz transducer, was firstly performed at 6h of age to detect IVH and thereafter at 24, 48, and 72h of age. PT pups with IVH were assigned in the IVH group, while those without a perceptible IVH at all time points were allocated to the control group.

Paper IV

Brain HFU (Visualsonic Vevo 2100, Visualsonics Inc, ON, Canada), using an MS-550D 40 MHz transducer, was performed at 8h and 24h of age to detect IVH *in vivo.* After that the HFU analysis was performed *ex vivo* as the following: brains were fixed in a small plastic tube to avoid movements and placed on an adjustable (y- and

x-axis) plate. The MS-550D 40 MHz transducer was fixed with a transducer holder on a bench-mounted adjustable rail system (Visualsonics Inc, ON, Canada), allowing changes in insonation position in all three directions. The transducer was positioned well anteriorly of the ventricular system and then moved in a posterior direction until the ventricles began to appear. Two-dimensional HFU images were obtained every 1000 μm.

Paper V

Brain HFU imaging (Visualsonic Vevo 2100, Visualsonics Inc, ON, Canada), using an MS-550D 40 MHz transducer, was performed at PND 1 and PND 2 to detect and grade IVH. PT pups with IVH were assigned to the IVH group, while those without detectable IVH on HFU were used as controls.

To confirm the presence of PHVD an *ex-vivo* brain HFU was also performed directly after the termination. At PND 33 the cranial sutures were completely fused, therefore an artificial ultrasound window was created.

Brain HFU provides an excellent possibility to detect the presence of IVH and follow its evolution into PHVD in real-time. Similar to human PT infants, the procedure of HFU in PT rabbit pups is quick and pain-free. The validation of HFU was elegantly performed and described in PT rabbit pups (114), making it a reliable tool to use. Moreover, given a great resolution (approximately 30 microns) at 40 MHz frequency, it allows very detailed visualization of the brain structures. Moreover, thanks to the availability of HFU intracerebroventricular injections may be performed under ultrasound guidance, limiting by that procedure-related injury. It should be mentioned though that higher frequency might be potentially harmful through thermal and mechanical biomechanism (138,139), however, the safety data currently available are controversial (139,140). The little safety data available point out the HFU exposure time, which may induce the neuronal migration alteration if lasting more than 30 minutes (139,140). In our studies, the exposure time of HFU in vivo was approximately 4 min.

Magnetic resonance imaging (MRI)

Paper IV

Brain MRI was performed using a 9.4 T Agilent magnet equipped with Bruker BioSpec AVIII electronics and a BGA-12S HP gradient system with a maximum gradient strength of 673 mT/m. A 075/040 mm diameter Bruker transmit-receive volume coil was used. Samples were dissolved in phosphate-buffered saline and fixed with a plastic holder in a 50 ml centrifugation tube. High-resolution three-dimensional T2 weighted brain images were acquired by a 2D EPI sequence as

follows: Echo Time (TE) = 34 ms, Repetition Time Repetition (TR) = 6.2 s, 0.3 mm slice thickness with no interslice gap, 125-140 coronal slices, in-plane acquisition matrix of 93 × 93 and Field of View (FoV) of 28 x 28 mm^2, resulting in a voxel dimension of 0.3 × 0.3 × 0.3 mm^3. Acquisition time was 26.5 minutes. Diffusion-weighted images (DWI) were obtained by a standard 2D EPI diffusion sequence covering 256 gradient directions with a b-value of 3000 s/mm^2 simultaneously with six references (b = 0) images. Additional experimental parameters were: TE = 33 ms, TR = 6.2 s, slice thickness = 0.4 mm with no interslice gap, 94 -109 coronal slices, in-plane acquisition matrix of 70 × 70, FoV of 28 × 28 mm^2, resulting in a voxel dimension of 0.4 × 0.4× 0.4 mm^3. The entire scan time for both acquisitions was 4 h 3 min 2 s.

MRI is considered to be a "gold standard" for the detection of brain damage therefore it was used to evaluate the accuracy and reliability of HFU- based ventricular volume reconstruction. Considering few data available on rabbit brain MRI below PND 7 and different Agilent magnet used, we needed to establish our protocol for the current study. Using the 2D EPI sequence in our setup we achieved a very good contrast. However, the total acquisition time was 4 hours, which would not be feasible in a living animal.

Intracerebroventricular injections

Paper II

<u>A1M biodistribution study:</u> PT pups were randomized following brain HFU at 18h of age as follows: pups with detectable IVH were allocated either to IVH + human recombinant A1M (rA1M) group or IVH + Vehicle group. Thereafter, under the guidance of HFU, pups in IVH + rA1M group were administered with 25µl of rA1M (rA1M, 9.4 mg/ml, A1M Pharma AB, Lund, Sweden) *i.c.v.*, while IVH + Vehicle group pups received *i.c.v.* 25µl of vehicle solution (10mM Tris-HCl pH 8.0, 0.125M NaCl, A1M Pharma AB, Lund, Sweden). The injections were done using 27-G Hamilton needles (Hamilton Robotics, Reno, NV, USA).

<u>A1M functional protection study:</u> Following the detection of IVH by HFU, PT pups with IVH were randomized either to IVH + human (h)A1M or IVH+Vehicle. A1M was derived from human donor plasma for the current study. At approximately 8h of age, under HFU guidance, pups in IVH + hA1M group received *i.c.v.* 25µl of hA1M (9mg/ml), whereas IVH+Vehicle group pups received *i.c.v.* 25µl of sterile artificial CSF solution. The injections were done using 27-G Hamilton needles (Hamilton Robotics, Reno, NV, USA).

We chose intracerebroventricular injections to administer either rA1M or hA1M for several reasons. First, the mean body weight of PT rabbit pups on the 2nd day of life is approximately 39 grams with small subcutaneous veins rendering the execution

of intravenous administration very difficult. Secondly, there is no certainty yet if and to which extend A1M could pass BBB. Finally, the half-life time of A1M is very short, approximately 3 minutes (141).

Sex determination

Paper II and V

To detect the male sex, the molecular PCR (polymerase chain reaction) technique for the detection of SRY (specific region of the Y chromosome) sequences was applied. Fresh skin tissue was gathered at harvesting for DNA isolation using DNeasy Blood & Tissue Kit (Qiagen, Hilden Germany). One uL of DNA was used for PCR. Amplification of SRY fragment was employed in 30 cycles as follows: initial denaturation step 95 °C 3 min followed by 95 °C 30 sec, 57 °C 30 sec, 72 °C 1 min with last step 72°C 10 min using specific primers; left primer: TGCAATACAGGAGGAACACG, a right primer: AGCAAACTGTCGCTCTTCT. Obtained PCR products, 299 bp, were analyzed by electrophoresis in 1,7% agarose gel with SYBR safe DNA gel stain (Invitrogen) and visualized by Image Lab software (BioRad).

Neurobehavioral examination

The rationale for evaluating gait and coordination on an inclined surface and righting reflex derived from the previous observations in PT rabbit pups with IVH (113,142–148). Unlike previously reported results, where the evaluation was performed at PND 14, our examination took place at PND 30 resulting in advanced maturation.

Open field test examines the anxiety and global motor activity, which are very relevant to neurobehavioral disturbances related to IVH. Generally, it is the most widely used test in rabbits thereby providing the possibility to compare results with the other studies. Indeed, PT rabbit pups at PND 30 exhibited a higher anxiety rate compared to the term pups at the same age (129,138). However, OF behavior has not been previously evaluated in PT rabbit pups with IVH.

Another widely used neurobehavioural assessment in rabbits is ORT, which tests cognitive abilities and memory and it has not been performed previously in PT rabbit pups.

Paper V

Neurobehavioral testing was performed between PND 29 and 32 as previously described (138,149). Examiners were blinded to the condition of the animal during the testing (PHVD *vs* control). There were no visible differences in general animal

performance that allowed us to discriminate between the groups. The motor examination included muscle tone and strength, righting reflex, and gait. The assessment of muscle tone included active flexion and extension of forelegs and hind legs (score 0 to 3). The righting reflex was measured by the ability of and time taken for PT rabbits to turn from supine to prone position. Gait and coordination were examined by testing the PT pups´ ability to hold their position when placed on an inclined slope. The test was conducted on a white rectangular plastic surface (70x60 cm) placed at 60° inclination. Latency to slide down the slope was measured after placing the pup at the upper end of the surface.

The open field (OF) test and the object recognition task (ORT) were performed in an arena (140 cm × 140 cm; walls 40 cm) with a standardized light intensity across the arena, details below. The arena was cleaned with 10% ethanol solution after each session to remove any olfactory cues. The ORT was undertaken at different intervals. Tests were performed between 8 a.m. and 3 p.m. on four consecutive days in the following order: OF; ORT habituation; ORT 30 min inter-trial interval; ORT 240 min (outlined below).

Open field (OF) test: The rabbits were taken from their cage one by one wrapped in a clean cloth to minimize stress and introduced in a corner of the arena. The arena was subdivided into three zones: the central square "center", the outer rim "peripheral zone" and in between the "intermediate zone." The 5 minutes latency to leave the starting point and time spent in each arena area were measured.

Object recognition task (ORT): Two objects were placed within the arena, 60 cm apart and 40 cm from the walls of the arena. The weight of the selected objects did not allow the rabbits to move or to jump and sit on the objects. Rabbits were taken out of their cage wrapped in a clean cloth and placed in a smaller cage for 5 min (L x W x H = 42cm x 19cm x 27cm) after which time each rabbit was introduced into the arena in one of the corners. The ORT consisted of three phases: the familiarization phase (T1; 5 min) and a test (T2; 5 min), separated by an inter-trial interval of 5-, 30- and 240-min on testing days 2, 3, and 4, respectively. To allow the rabbits to habituate to the experimental settings, the first two sessions were considered as training. Following the familiarization phase (T1; 5 min) during which the rabbit could freely explore the arena and interact with 2 identical objects, the animal was returned to its cage for 5, 30, or 240 min. Before the test phase (T2; 5min), one of the 2 objects used in the T1 phase was replaced with a clean identical object, while a novel, distinct object, replaced the second object used in T1. The side of the arena (either right or left) of the novel object was randomized to prevent the side preferences. Each object was cleaned with 10% ethanol before and after each session to eliminate any olfactory cues. Different combinations of objects were used in a balanced manner to minimize potential bias due to preferences for a particular object. Exploration of the objects throughout T1 and T2 was defined as

touching or sniffing while pointing towards either object within a distance of <2 cm. Exploration indices "E1" and "E2" were calculated as the cumulative time to explore the objects during T1 and T2, respectively. For T2 only, "D1" reflected the difference in time exploring the old and novel object whereas "D2" (discrimination index) was calculated as (D1/E2). Rabbits were excluded from the analysis in case of absent exploration of any object during T1 or T2.

Brain tissue sampling and processing

Paper I

At 72h of age rabbit pups were anesthetized by isoflurane (1000 mg/g, Virbac Carros, France) and terminated by transcardial perfusion-fixation with saline (PBS, pH 7.4) and freshly prepared 4% paraformaldehyde (PFA, VWR Chemicals, Leuven, Belgium, buffered with PBS, pH 7.4) for histochemistry, immunolabeling, and scanning electron microscopy (SEM). Three- to 6h later a change to a fresh 4% PFA was done. Brains were thereafter cryoprotected by sequential immersion in 15% sucrose for 6h and 25% sucrose for another 6h. Brains were mounted in TissueTec (Sakura Finetek, Torrance, CA, USA) and frozen (at around -60°C) in cryomolds, on dry ice in isopentane. Sections (12μm) were cut on a cryotome (Microm, HM 500 OM, Microm Laborgeraete GmbH, Walldorf, Germany). Sections were collected on superfrost plus slides, two per slide, starting from the end of the olfactory bulb to the end of the midbrain. Sections were stored at -20°C until used for the labeling.

Paper II

Rabbit pups were sedated with *i.p.* ketamine injection (35mg/kg, Intervet International BV, Boxmeer, The Netherlands) and isoflurane inhalation anesthesia (1000 mg/g, Virbac Carros, France). Transcardial perfusion-fixation with fresh saline (PBS, pH 7.4, containing 0.01% of heparin) and freshly prepared 4% PFA (PFA, VWR Chemicals, Leuven, Belgium, buffered with PBS, pH 7.4) was performed. Brains were then dissected out from the skulls and immersed in 4% PFA. Six- to eight hours later a change to fresh 4% PFA was done, followed by immersion in 4% PFA, at 4°C. Subsequently, brains were sequentially immersed in 10% sucrose and 20% sucrose for cryoprotection for a total of 16h. Brains were then mounted in TissueTec (OCT, Sakura, Japan) and frozen (at around -60°C) in cryomolds. Sections (12μm) were cut on a cryotome (Microm, HM 500 OM, Microm Laborgeraete GmbH, Walldorf, Germany) and collected on superfrost plus slides, two per slide, starting from the end of the olfactory bulb to the end of the midbrain. Sections were stored at -20°C until used for the labeling.

Tissue collection and processing for mRNA and proteins: rabbit pups were terminated either at 24 or 72 h of age. Brains were quickly dissected out from the

skulls and sectioned at the level of the midseptal nucleus. A 1-mm section around the periventricular zone was dissected, snap-frozen, and stored at − 80 °C until further mRNA and protein analysis, as described in paper II.

Paper IV

The non-perfused brains from rabbit pups with previously performed brain HFU *in vivo* (18 IVH and 4 controls) and who died spontaneously at 24 - 48 h of age were used for this study. Extracted brains were immersed and preserved in 4% PFA (PFA, VWR Chemicals, Leuven, Belgium, buffered with PBS, pH 7.4) until neuroimaging was performed. Twenty-four hours before the acquisition of the images the brains were rinsed in phosphate-buffered saline and fixed in centrifugation tubes.

Paper V

Rabbit pups were sedated with *i.p.* ketamine (35mg/kg, Intervet International BV, Boxmeer, The Netherlands) and xylazine (6 mg/kg, VM Pharma AB, Sweden), followed by transcardial perfusion-fixation with saline (PBS, pH 7.4, containing 0.01% of heparin) and freshly prepared 4% PFA (PFA, VWR Chemicals, Leuven, Belgium, buffered with PBS, pH 7.4). The brains were post-fixed by immersion in 4% PFA. Brains were dehydrated in a graded ethanol serial (70–99.99%) and Xylene (100%) and embedded in paraffin blocks. Coronal sections (5 μm) were cut on a rotating microtome (Microm HM 360, Microm International GmbH, Walldorf, Germany), and sections were collected on microscope slides (SuperFrost Plus, Thermo Scientific/Gerhard Menzel B.V. & Co., Braunschweig, Germany). Sections were incubated in cresyl violet solution (0.1% in H20) followed by dehydration (ethanol serial ended with Xylene) and mounting (in Pertex).

There was a slight methodological difference in brain perfusion protocol between paper I and papers II and V. Namely, we added heparin to PBS for a better washout of intravascular blood components to improve the flow of fixative, resulting in better tissue fixation quality (150).

The brains in paper IV were fixed by immersion into 4% PFA solution. We did not choose the ex-vivo perfusion-fixation because the results could be suboptimal, raising the risk for mechanical brain tissue damage as it was described previously (150). Furthermore, we planned to use these brains for neuroimaging studies to assess the ventricular system and the immersion fixation, in this case, was sufficient, while for immunohistochemical evaluation, perfusion-fixation in vivo should be done for the optimal assessment of all brain structures (150).

A comprehensive review on IVH-related WM injury in pre-clinical and clinical studies

We searched for the relevant preclinical and clinical studies in the following databases: MEDLINE via PubMed (1966 to April 30, 2019), Embase (1980 to April 30, 2019), and clinical trial databases. We included preclinical studies with a control group assessing WM damage following IVH; randomized clinical trials on the same topic were included.

Analysis

Neurobehavioral assessment

Paper V

For neurobehavioral assessment, the animal position was automatically registered by a PC connected to a video camera, installed 250 cm over the field. To analyze the images Video Tracking Software (SMART, Panlab SL, Barcelona, Spain) was used. The authors were blinded to animal group assignment throughout testing, data gathering, and analysis.

Volumetric reconstruction of the ventricles

Paper IV

HFU

The right and left lateral ventricle volumes were measured using an in-house developed MATLAB program (MathWorks Inc, Natick, MA, USA). On each HFU image, starting from the most anterior portion of the lateral ventricle proceeding to the most posterior part of the ventricle, the right and left lateral ventricles were manually delineated. The volumes of the right and left lateral ventricle were estimated by calculating the sub-volumes between two HFU images using the MATLAB function convhull (The MathWorks Inc, USA) by combining the delineation of the two HFU images. When all sub-volumes were calculated the total volume was summarized up. Detailed description in paper IV.

Although the spatial resolution of HFU is excellent, the contrast between the two types of tissue may be limited. To calibrate our method we developed a phantom made by ballistic gel (Clear Ballistics LLC, Arizona, USA) with a butter inclusion

of known volume. By iteration between the blinded operator and the engineer, we were able to calibrate our model.

MRI

Osirix MD 8.0 (Pixmeo SARL, Switzerland) was used to analyze the images. Manual delineation of each (right/left) lateral ventricle was done separately: every second slice was delineated and, following the delineation of the whole ventricle, the software reconstructed the ventricular volume

Periventricular brain tissue

Selection of anatomical brain regions

Paper I

To describe neuroanatomy of the brain, thus facilitating the selection of comparable levels from all rabbit brains for histochemical and immunolabeling analysis, hematoxylin-eosin (HE) staining was performed on every 10-15th section. The detailed HE staining procedure is reported in Paper I.

Papers II and V

The HE staining protocol for the definition of neuroanatomical regions and levels suitable for the analysis, as described in Paper I, was also adapted for Papers II and V.

We chose four different neuroanatomical levels representing rostral (level 1) and caudal (level 2) forebrain, rostral (level 3), and caudal (level 4) midbrain for all the studies (Figure 10). By choosing these four levels we could achieve a detailed overview of the brain structural changes, revealed by immunohistochemical staining, induced by IVH throughout the brain. Moreover, the pre-specified levels across the studies underscored the consistency of the results. We followed "Atlas of the rabbit brain and spinal cord" for neuroanatomical nomenclature (151).

Peroxidase Histochemistry

Paper I and Paper II

To identify peroxidase (PO) activity as the result of the presence of extracellular Hb, thereby defining its distribution within the brain WM in both groups (IVH and control), we adapted a protocol of the enhanced peroxidase reaction on cryosections (Strum 1970). Every 10th section was stained for PO, matched with HE stained sections, and immunolabeled sections including the selected regions of interest (ROIs) at the comparable levels. The procedure is described in detail in Paper I.

One could argue that background PO staining might be caused by tissue endogeneous PO activity. In fact, to rule out this possibility we performed, as controls for the PO staining, pre-incubation of the sections in H_2O_2, which leads to irreversible inactivation of endogenous peroxidase.

Immunofluorescent labeling for Hb and rA1M

Papers I and II

To specifically detect Hb for comparison with PO activity, we performed single immunofluorescence (IF) labeling of Hb, of selected ROIs. Double IF labeling with polysialic acid neural cell adhesion molecule (PSA-NCAM), a marker of developing and migrating neurons and of synaptogenesis, was performed to further elucidate the distribution of Hb in differentiation zones and regions of plasticity following IVH. This was performed as described in papers I and II.

Single immunofluorescence (IF) labeling of Hb was implemented to explicitly detect Hb for comparison with the PO activity of selected ROIs. We performed a double IF labeling with polysialic acid neural cell adhesion molecule (PSA-NCAM), a marker of neuronal plasticity and synaptogenesis, to investigate the distribution of extracellular Hb in differentiation areas with high neuronal plasticity following IVH. The procedure is described in detail in Papers I and II.

Paper II

To determine if rA1M could be possibly detected in brain tissue following *i.c.v.* administration and consequently compared amid the experimental groups and linked to the PO activity, immunohistochemistry labeling (IHC) of rA1M was done. IHC for rA1M was performed on cryosections from the IVH+rA1M animal group parallel to those used for the PO staining. The detailed protocol of IHC for rA1M is described in Paper II.

We performed rA1M immunofluorescent labeling in adjacent sections as for PO and A1M IHC to define the specificity of rA1M labeling. Additionally, to investigate whether rA1M could have a similar distribution pattern as extracellular Hb in brain high plasticity areas, we performed double IF labeling with PSA-NCAM. A detailed description of IF labeling is reported in Paper II.

Electron microscopy

To evaluate the presence of intact RBCs scanning electron microscopy (SEM) at high magnification was used. Moreover, it helped to distinguish the areas of cellular and non-cellular PO-activity. The procedure was implemented on cryosections containing the selected ROIs from both groups of animals (IVH and control), as described in Paper I.

Transmission electron microscopy (TEM) and TEM-IHC were used to elucidate the impact of IVH on the mitochondria structural integrity and the expression of tumor necrosis factor-alpha (TNFα). To detect whether hA1M may have a protective role following IVH a similar analysis was performed in the IVH + hA1M animal group, as described in paper II.

NeuN, Synaptophysin, Myelin basic protein and GFAP in selective brain regions

To evaluate the immunoreactivity of NeuN-positive neuronal bodies, GFAP-positive cells and fibers, MBP and synaptophysin immunoreactivity in denoted ROIs (*amygdala, nucl. caudate, corpus callosum, internal capsule,* and *hippocampus* with subregions CA1 and *gyrus dentatus*) the respective IHC labelings were performed as described in detail in paper V.

These specific antibodies were chosen based on previous reports of reduced neurogenesis, astrogliosis, and reduction in myelination in the PT rabbit pups with IVH at PND 14 (142–144,146–148,152) and in human PT infants with IVH post-mortem studies (83,153), underlying the relevance of their analysis.

Myelin organization analysis

The rationale to perform myelin organization analysis was based on the hypothesis that IVH/PHVD leads not only to hypomyelination but also to alteration of myelin microstructure. Recently, this analysis was validated in four different brain injury models in rodents (a rat and a mouse model of neonatal diffuse WM injury, a mouse model on neonatal asphyxia, a rat model of neonatal stroke) and it has been demonstrated to be sensitive to detect even subtle changes in myelin microstructure (154).

To quantify the relative amount of myelin and organization of the WM microstructure, ImageJ was used to analyze the relative area coverage of myelin and apply the publicly available plugin (https://doi.org/10.1088/1758-5090/aa6204). This approach uses a theoretical framework to break the image into segments and measure the vector of each segment (Directionality) and assess the variance in this organization (Dispersion); the detailed description in paper V.

Cortical layering, PV-positive interneuron and PNN

To define cortical layers, PV positive interneurons and PNNs a standardized IF protocol was conducted as described by Stolp (84). For both stains, ROIs were

extracted from the medial and lateral sides of the parietal cortex from both the left and right hemispheres.

For cortical layering analysis, layer measurement was standardized by drawing a polyline (segmented at one point in the approximate center) at the start of layer I that spanned 2mm of the cortex. The line was duplicated and lowered until reaching 3 intense NECAB1+ cells that represented the start of layer IV and this distance represented the length of layers I-III. Again, the segmented line was duplicated and lowered until it reached cortex absent in NECAB1+ cells representing the end of layer IV. This was repeated for measuring layers V-VI, where the end of layer VI was defined by the absence of CTIP2+ cells.

For interneuron analysis, ROI's were extracted as described for cortical layering analysis, and PV immunoreactive cells were counted manually; WFL-positive PNNs were defined as an entire halo encompassing a PV-positive interneuron. See detailed description in paper V.

RNA Isolation and Real-Time PCR

Paper II

RNA was extracted from periventricular tissue using the acid guanidinium phenol-chloroform method and RNeasy Mini kit supplied by QIAGEN (Germantown, MD, USA). Reverse transcription was conducted following the manufacturer's instructions on 0.1-1µg total RNA using the iScript cDNA synthesis kit (Bio-Rad, Hercules, CA, USA) and the RT^2 First-strand kit (QIAGEN). RT^2PCR Profiler Array real-time PCR (custom made by QIAGEN) was applied to quantify the mRNA expression of TLR-4, monocyte chemoattractant protein-1, IL-1β, IL6, IL8, IL1 receptor(R) 1, TNFα, MMP-9, heme oxygenase-1. Data were normalized to glyceraldehyde-3-phosphate dehydrogenase (GAPDH, a primer from QIAGEN), with fold change values calculated by normalizing against sham control animals.

Statistics

Paper II

ANOVA with post hoc Bonferroni was used for comparisons between multiple groups. P-value was set at <0.05 significance level.

Paper IV

The analyses were performed using Matlab. All acquired data were tested for normality of distribution using the Lilliefors test. Group data were reported as means

and standard deviation (SD). The agreement between the HFU and MRI was evaluated by intraclass correlation coefficient (ICC) (if the data was normally distributed), coefficient of variation (CV), Bland–Altman analysis, and linear regression using Pearson correlation coefficient. The ICC estimated the degree of absolute agreement for a single measurement or average of two independent measurements on randomly selected objects. In the ICC analysis only brains with PHVD were included to obtain a population with a normal distribution.

The agreement between the methods was evaluated using the mean of two measurements for the respective lateral ventricles examined by HFU and MRI respectively.

To test the intra-observer reliability, repeated HFU- and MRI-based measurements of lateral ventricular volume were performed at two different time points. The period time between the two investigations was between 4 - 6 months. The investigator was blinded to the values obtained at the first time-point.

Paper V

We performed the statistical analysis by using Mann–Whitney and Wilcoxon's signed-rank test, respectively, for independent and paired continuous variables to compare each group to the reference. A one-tailed t-test was applied for the ORT analysis to compare D2 scores with chance level (D2 = 0). P-value <0.05 was considered statistically significant. Results are presented as mean (standard deviation) or median (interquartile range or CI95%). The analyses were performed using SPSS (PASW Statistics 18, IBM, Deutschland GmbH) software.

For cortical layering analysis, to assess treatment *vs* control effect on total cortical depth (Layers I-VI), the analysis was conducted using an unpaired student's *t-test*. Grouped data of layer depth (I-III, VI, V-VI; IVH *vs.* control) were analyzed using two-way ANOVA, and when statistical significance was attained for treatment *vs* control, *post hoc* analysis was performed with Sidak's multiple comparisons. For interneuron and PNN analysis, grouped data were analyzed using two-way ANOVA, and where significance was obtained, subsequent *post hoc* analysis was conducted with Sidak's multiple comparisons. For all analyses, $p<0.05$ was indicative of statistical significance. For myelin analyses, we used an unpaired Student's t-test following ascertainment that the data were normally distributed. For cortical layers, PNN, interneuron, and myelin organization statistics were undertaken with GraphPad Prism (9.0, San Diego, CA, USA).

Results and comments

Paper I

Extracellular Hb is distributed throughout periventricular WM following IVH in the preterm rabbit pup.

Hypothetical statement

We assumed that following IVH there is a disruption in ventricular ependymal lining allowing extensive amounts of RBCs and extracellular Hb to penetrate periventricular WM.

Findings and discussion

The results of this study confirmed the hypothesis that following IVH in PT rabbit pup there is a breach in the ventricular ependymal lining leading to a wide distribution of extracellular Hb throughout periventricular WM. Consistent with our previous studies, we detected a rapid development of PHVD within the first 3 days of life following IVH in PT rabbit pups. We observed a widespread distribution of RBCs in all neuroanatomical ROIs from the frontal areas of the rostral forebrain to the posterior areas of the caudal midbrain by HE staining (Figure 9.A.). The most pronounced presence of intact RBCs was in the occipital parts of the brain (rostral and caudal midbrain), particularly in distended CP, subfornicular organ (SFO), and also in three circumventricular organs. Additionally, the presence of RBCs was found in the thalamus and hippocampus.

Correspondingly, PO staining and immunolabeling of Hb confirmed the presence of extracellular Hb in the same brain areas containing intact RBCs (Figure 9.B.). Furthermore, PO activity and Hb immunolabeling suggested the presence of non-RBCs related to Hb in cell bodies, in differentiation zones and axonal fiber tracts. Indeed, double immunolabeling with PSA-NCAM demonstrated a high co-existence of extracellular Hb in high plasticity WM areas. Besides, in the previous study by our group, it has been shown that due to ongoing hemolysis following IVH there is a continuous release of extracellular Hb into CSF, where it is auto-oxidized into metHb and it reaches peak concentration at approximately 72h following IVH onset (56). MetHb is known to be a potent pro-inflammatory inducer. In fact, MetHb concentration is correlated with an increase of TNF-α in CSF and an increase in TNF-α, IL-1β, and HO-1 mRNA levels in periventricular brain tissue 72h later of

IVH onset (56,62). Furthermore, it has been shown that extracellular Hb damages axonal myelin and OLs by triggering oxidative cascade (155). We show here that extracellular Hb reaches easily brain areas corresponding to corticospinal tract motor axons, damage to which reflects in spastic diplegia in infants with PHVD (156). The wide distribution of extracellular Hb at 72h following IVH is in line with the previous findings of our group, supporting the hypothesis of extracellular Hb being an inducer of different pathways resulting in WM and GM injury following IVH.

Interestingly, we observed positive staining for extracellular Hb within periventricular areas adjacent to a morphologically intact ependyma, suggesting the possibility of passive diffusion through the ependyma guided by a concentration gradient. However, we cannot exclude the possibility of an alternative diffusion pattern of extracellular Hb within periventricular WM following IVH. Further studies may elucidate the traveling pattern of extracellular Hb.

Furthermore, it has been shown that PT infants with IVH have reduced brain GM volumes (77). Considering extensive deposition of extracellular Hb within the subventricular zone and its capability to trigger oxidative stress and pro-inflammatory cascade, there is the possibility that it causes damage not only to glial cells progenitors but also alters the maturation and migration of interneurons (157,158). One could also speculate that such a wide distribution of extracellular Hb within brain WM may lead to axonal damage and retrograde neuronal degeneration resulting in decreased cortical GM volume.

52
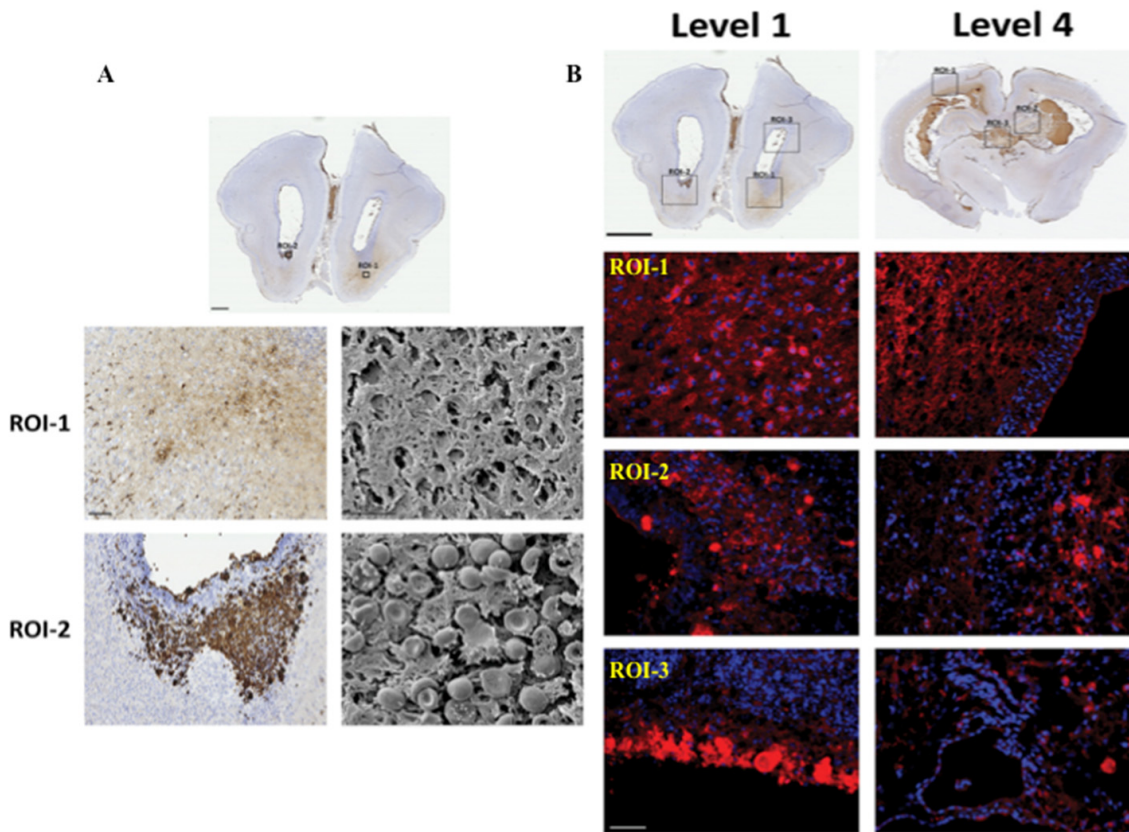
Figure 9. Distribution of intra- and extracellular Hb. A. The presence of RBCs and Hb following IVH in preterm rabbit pup using the inherent PO activity of Hb in combination with SEM. Scale bar for SEM images indicates 10 µm. B. Hb immunolabeling (red) of selected regions (ROIs) of PO activity corresponding areas recorded in parallel sections. DAPI labeled cell nuclei are blue. The scale bar of slide scan images is 2.5 mm and of ROI images indicate 25 µm.

Another finding of this study that should be mentioned is an extensive hemorrhage in the SFO area. Anatomically, SFO is located on the roof of the third ventricle and it plays an important role in osmoregulation and cardiovascular regulation by the control of the release of angiotensin and vasopressin (159). IVH in PT pups is induced by *i.p.* injection of glycerol, which results in dehydration, vascular hyperosmolarity, and thereby transmural pressure gradient leading to vessel rupture (122). To date, the infusion of hyperosmolar solutions in human PT infants is considered to be one of the risk factors inducing IVH (22). Further studies may elucidate the role of SFO in IVH development.

We suggest that following IVH, extracellular Hb, due to its highly cytotoxic properties, may be a central initiator of pathophysiological events leading to long-lasting brain damage, eventually resulting in neurodevelopmental or neurobehavioural impairment.

Paper II

Following *i.c.v.* administration, the heme and radical scavenger A1M is extensively distributed throughout the brain and cerebellum following IVH in the PT rabbit pup and appears to be protective by reducing mitochondrial damage and mRNA expression of pro-inflammatory and inflammatory signaling genes.

Hypothetical statement

Administration of A1M, a heme and radical scavenger, may protect from secondary brain damage following IVH in the preterm rabbit pup.

Findings and discussion

In line with the results from the paper I, similar PO activity was detected in all evaluated neuroanatomical regions following IVH in the PT rabbit pup. Accordingly, the presence of extracellular Hb was confirmed by IF staining of Hb in the periventricular WM and WM tracts.

Following IVH, *i.c.v.* administration of rA1M resulted in a broad distribution of A1M within periventricular WM and fiber tracts and even in WM of the cerebellum, as observed by IHC (Figure 10. A.). Double IF labeling for A1M and Hb confirmed a co-existence and even co-localization at the cellular level within periventricular WM, fiber tracts, thalamic region, corpus callosum, corona radiate, and hippocampus (Figure 10. B.). Additionally, double IF labeling of A1M and PSA-NCAM demonstrated a distinct co-existence within periventricular and cerebellar areas with high plasticity (WM, subventricular zone, corpus callosum, corona radiate, thalamocortical projection).
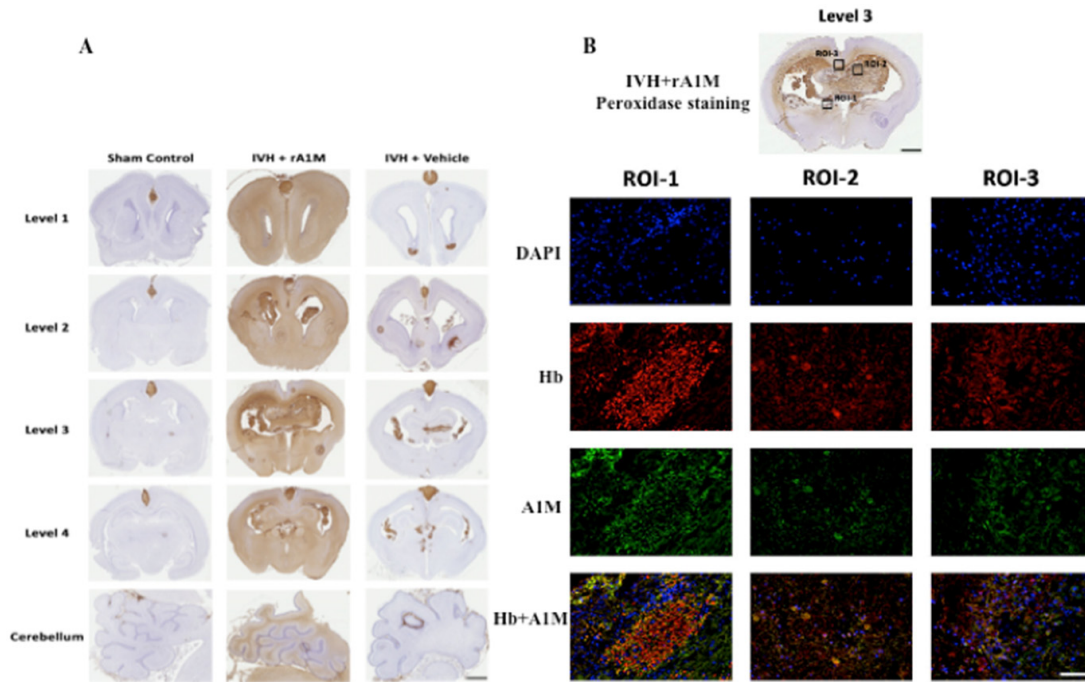
Figure 10. Distribution of rA1M throughout the brain following IVH in preterm rabbit pup. A. The distribution of *i.c.v.* administered rA1M within the brain extending to the cerebellum in PT pups with IVH, whereas no A1M was detected in sham control and IVH+Vehicle group animals. Scale bar indicates 5 mm and is applicable for all images. **B.** Images show the double IF labeling for Hb (red) and A1M (green) together with the nuclear staining DAPI (blue) in animals with IVH treated with *i.c.v.* injections of rA1M (IVH+rA1M). The scale bar of slide scan images indicates 2.5 mm and in ROI images 25 µm.

We suggest though, that rA1M has a similar distribution pattern as extracellular Hb. The exact mechanism for such a spreading of A1M and extracellular Hb is unclear. However, diffusion-MRI studies indicate the diffusion of water molecules both in damaged brain tissue (160,161) and in relation to brain activity (162,163). Moreover, the diffusion of water molecules is faster in WM fiber tracts which may be related to gradient pulse direction (160). PHVD develops rapidly over 72h in the PT rabbit pups following IVH, suggesting that there might be disruption of periventricular WM integrity allowing for diffusion of even larger molecules such as extracellular Hb and A1M, towards a concentration gradient following IVH. Indeed, rA1M was found in cerebellar WM, in line with the findings by Agyemang (75).

Importantly, i.c.v administered hA1M preserved structural integrity of mitochondria, attenuated up-regulation of pro-inflammatory markers, cellular response, oxidative stress, and matrix degradation proteins, as demonstrated by EM-IHC and RT-PCR analysis. The apparent neuroprotective function of A1M is believed to be related to its reductase properties, free heme, and radicals scavenging (98,164,165), thereby confirming the hypothesis that extracellular Hb metabolites may have a central role in IVH-related secondary brain damage. However, the exact mechanisms whereby exogenous A1M protects following IVH are unknown.
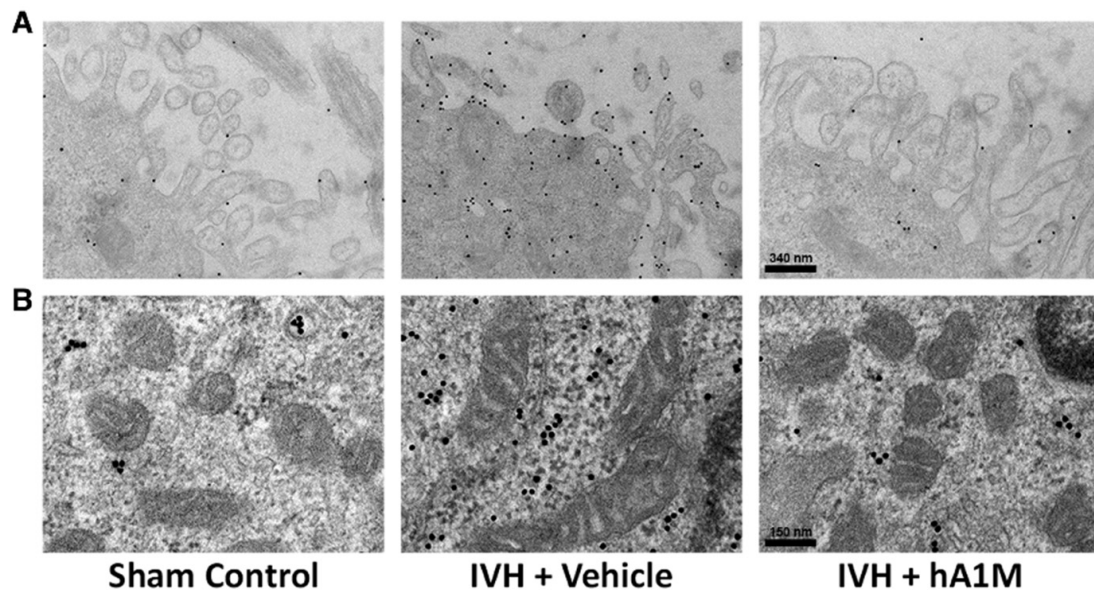
Figure 11. hA1M reduces structural damage and mitochondrial hypertrophy. Rabbit pups with confirmed IVH injected *i.c.v.* with hA1M (IVH + hA1M) or Vehicle (IVH + Vehicle) or Sham Control (no bleeding as confirmed with HFU) were euthanized at 72 h of age. Scale in the top panel (a) indicates 340 nm and in the lower panel (b) 150 nm.

The results of this study suggest that rA1M may be a potential candidate for neuroprotective treatment against brain damage following IVH. Our study was limited to 72h assessing the early functional effects of administered A1M. We detected the changes on the mRNA level, but we could not perform the analysis to determine corresponding changes on protein level due to lack of available material. Notably, the changes on mRNA level do not always reflect the respective changes at the protein level. Taken together, several unanswered questions should be addressed in future studies.

Paper III

A comprehensive review of available preclinical and clinical studies on IVH-related WM injury may help to identify research gaps and the effects of different types of interventions.

Findings and discussion

Due to the complexity of IVH disease, a variety of animal models have been employed to explore causes and mechanisms leading to IVH-induced brain injury. Most preclinical studies are focused on the treatment of IVH rather than prevention. The majority of animal models use animals born at term with mature systemic physiology and varying degrees of brain maturity, ranging from GA 24 weeks (PT rabbits, PT primates) to GA 34 weeks (piglets, rodents) when compared to human infants. The full-term delivery in some animal models neglects the interplay

between influential aspects of prematurity, such as trophic deprivation and coagulation impairment, as well as bleeding in the immature brain (spontaneous IVH was reported in PT rabbit pups (113) and PT primates (82)). With this major shortcoming in mind, these models still furnish substantial information concerning IVH and its related secondary brain injury development, together with possible treatment strategies.

Injection *i.c.v.* of centrifuged blood containing high hematocrit is one of the most used models to induce IVH in rodents and piglets, investigating the role of blood components in PHVD formation and WM damage (105–109).

Another way of inducing intracranial hemorrhage in rodent models is the stereotactic injection of collagenase into the germinal matrix. Collagenase dissolves the extracellular matrix encircling the capillaries, thereby opening the BBB, and leads to intracranial hemorrhage (110,111,127). It seems that neurocognition in the collagenase model is affected comparably manner to human infants. Moreover, similar to human infants, hemorrhage resulted in brain volume reduction (111,127).

Several risk factors such as the lack of cerebral blood flow autoregulation, rapid volume expansion, and hypercarbia, increase the risk for the appearance of IVH in PT infants (15). Indeed, this was supported by studies in newborn beagle pups in which induction of circulatory hypotension followed by rapid volume expansion led to IVH (17–19), having an important impact in clinical practice by raising the awareness of clinicians to provide as gentle care as possible following PT birth by avoiding rapid volume expansions and extensive and rapid fluctuations of carbon dioxide levels.

The only small animal IVH model utilizing PT-born animals is the rabbit IVH model, where bleeding is induced by *i.p.* injection of glycerol, leading to intravascular hyperosmolarity and rupture of the vessels within the germinal matrix (114,120,122). In the PT rabbit pup IVH model, both behavioral deficits and morphologic changes have been reported, such as neuroinflammation, periventricular cell death, PreOL death, the arrest of myelination, and axonal damage, reduced neurogenesis (113,142–144,146–148,152). Furthermore, the role of extracellular Hb was described in this model (56,62,166).

Several treatment strategies have been tested in these animal models, as targeting TLR_4 and SPAK pathways (34,167) and blockage of AQP_I to reduce the CSF hypersecretion (37,38), using extracellular Hb scavengers (66,75,168–171), suppressing ferritin up-regulation by minocycline (172–174), targeting PAR-$_I$ system (46), inhibition of metalloproteinases (48,49), targeting TGF-β (50,52). Of note, several clinical studies have been completed on possible treatment strategies. The DRIFT (drainage, irrigation and fibrinolytic therapy) study showed improved neurodevelopmental outcome and reduction in death or severe disability at 2 and 10

years of age in PT infants with severe IVH and PHVD respectively (12,39). However, this study was stopped due to a high rate of secondary bleeding and mortality in the treatment group (8). Another clinical trial in PT human infants with IVH tested the combination of two diuretics: acetazolamide (a carbonic anhydrase inhibitor) and furosemide (a Na/Cl co-transport inhibitor) (175–177). The reduced CSF secretion was achieved by this therapeutic strategy, however, the need for ventriculoperitoneal shunt placement remained unvaried. Most importantly, this treatment exacerbated neurologic morbidity.

In addition to the studies focusing on the attenuation of IVH-related secondary brain injury, others explore the opportunity of augmenting the repair of damaged tissue. The main strategies have focused on enhancing neurogenesis by administrating recombinant erythropoietin (178–180), melatonin (181,182), stem cell therapy (183–185), and reversal of hyaluronan build-up (143).

Although it is complicated to prevent IVH in PT infants, administration of insulin-like growth factor 1 (IGF-1) in complex with IGF binding protein-3 (IGFBP-3) might diminish the incidence of severe IVH in extremely PT infants (186), likely due to a maturational effect of administered IGF-1/IGFBP-3 on germinal matrix vasculature.

Delayed umbilical cord clamping is another intervention, performed immediately after birth, that has been demonstrated to reduce significantly the occurrence of IVH in PT infants (20). One could hypothesize that delayed umbilical cord clamping leads to an increment of circulating blood volume, thereby providing a stabilizing effect on cerebral blood flow. Furthermore, it may have an enhancing impact on the BBB by transfusing growth factors, coagulation factors, platelets, stem cells, exosomes, micro-vesicles, anti-inflammatory substances, and Hb scavengers. Animal studies of delayed umbilical cord clamping may investigate the mechanisms involved in abating the risk of IVH.

This review summarizes the body of evidence on preclinical and clinical studies on IVH-related WM injury. Systematic reviews of both preclinical studies and randomized clinical trials are important to assess the benefits and harms of different interventions to highlight research gaps and to avoid unethical research and waste of resources.

Paper IV

Volumetric reconstruction of ventricular size using HFU is highly accurate as compared to MRI and may be a promising non-invasive tool for evaluating the progression of post-hemorrhagic ventricular dilatation in the preterm infant.

Hypothetical statement

We proposed that HFU is an accurate and reliable tool for the reconstruction of ventricular volume in PHVD in the PT rabbit pup.

Findings and discussion

Volumetric reconstruction of brain lateral ventricles in PT rabbit pups using HFU was at least as precise as that of MRI: Pearson correlation coefficient between HFU– and MRI–based measurements was r = 0.99; ICC analysis showed an excellent correlation, being 0.994 (CI = 0.969–0.998) and the CV between the two methods was 3.2%.

The Bland-Altman plot (Figure 12) showed a good agreement between the two methods with a low bias for HFU–based lateral ventricle volume reconstruction confirming the accuracy of HFU–based measurements. These findings are encouraging and open up the perspective of performing HFU–based ventricular volume measurements in several clinical situations where MRI-based measurements are not possible due to patient instability as well as to infrastructure- and cost-related issues.
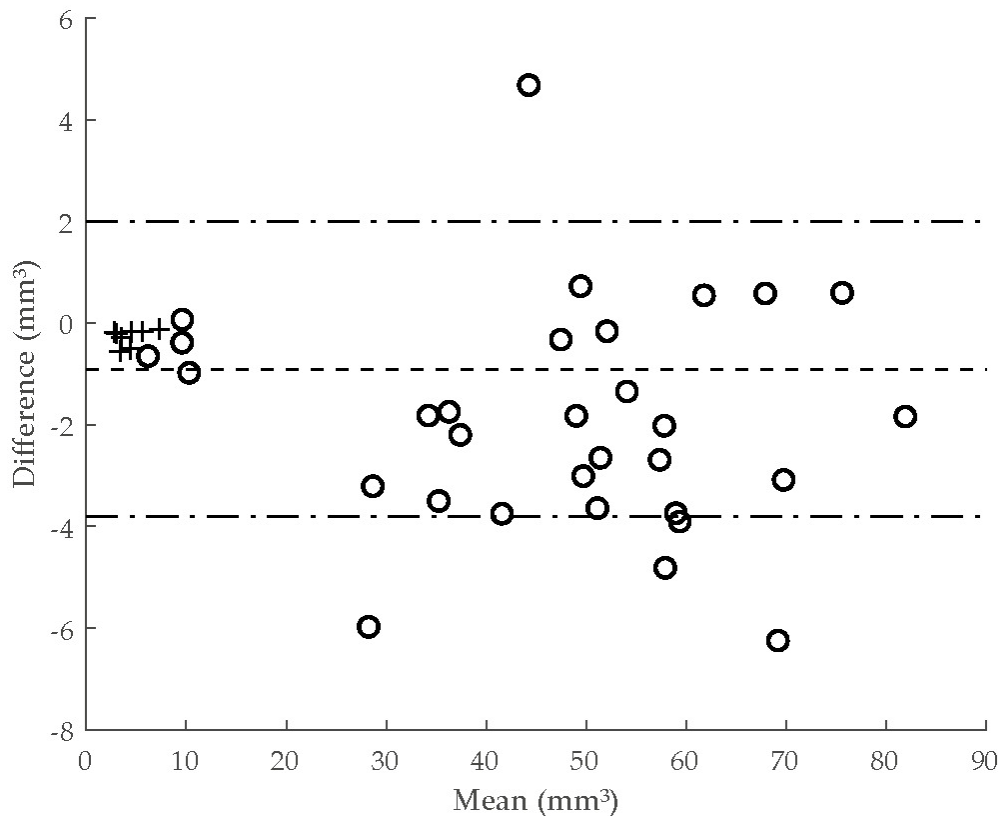
Figure 12. Absolute difference plotted against the mean of measurements of lateral ventricular volume comparing HFU and MRI for ventricular volumetric evaluation. The dashed curve shows the systematic difference. The dash-dotted curves show systematic difference ± 1.96 random difference, i.e., the 95%-confident interval. "+" – no IVH; "O" – IVH.

Importantly, volumetric reconstruction of ventricular size using HFU was highly repeatable with high intra-observer reliability, which suggests that HFU can be a precise clinical tool with a high reproducibility if performed by an experienced examiner. Currently, the evolution of PHVD in human PT infants is followed by 2-D cranial ultrasound, as well as the decision when to intervene to alleviate ventricular dilatation and intracranial pressure is made based on 2-D sonographic measurements (28). The enlargement of the ventricular volume results in an increase in intracranial pressure and injury to adjacent preriventricular WM (32), it would be very valuable therefore to have the possibility to estimate ventricular volume more precisely. Moreover, recently it has been demonstrated that a combination of several 2-D ultrasound-based measurements was less accurate in cases of large ventricular dilatation (187). Utilizing ultrasound-based 3-D measurements of ventricular volume raises the possibility of earlier intervention with a potential reduction of periventricular tissue damage due to ventricular dilatation. However, due to the scarce data available, further studies are needed to provide evidence that newborns with PHVD will benefit from ventricular volume measurements in decision-making on clinical intervention.

Interestingly, as in human PT infants (188,189), we observed that the volume of the left lateral ventricle was larger compared to that of the right lateral ventricle in PT rabbit pups. The reason for this asymmetry is still unknown. These findings underscore the validity of our PT rabbit model of IVH. The present findings obtained in the PT rabbit pup model are thus valid for translation to the clinical scenario of PHVD in PT human infants.

Compared to conventional ultrasound probes used in clinical settings (2-15 MHz) with a spatial resolution of approximately 100 -200 microns, a 40 MHz HFU probe, the frequency used in our study, has a depth of penetration of approximately 10-11 mm. This depth is excellent for visualization of the PT rabbit pup brain but insufficient for the examination of deeper structures in the human PT brain (135).

Moreover, the use of higher frequencies may raise the safety question. The potential harms related to ultrasound imaging may be induced by thermal and mechanical biophysical mechanisms. Indeed, FDA provides the recommendations on maximum acoustic output exposure levels (190). Higher ultrasound frequencies have a higher absorption rate and therefore may affect thermal and mechanical indices at larger amplitude. Thus, it is important to limit examination time, especially if applying higher frequencies. Although ultrasound is widely used in everyday clinical activities and animal studies, the data on safety are controversial and scarce.

It should be mentioned, that we performed all neuroimaging measurements *ex vivo* in non-moving objects, thereby optimizing the recordings by the exclusion of any movement artifacts. Furthermore, our study was limited to 48 h and did not address repeated measurements over time as opposed to the clinical situation where ventricular dilatation evolves over a longer time requiring repeated measurements of ventricular size. Another limitation of our study was the absence of inter-observer reliability. This was partly the reason why we chose to perform ICC analysis of the test-retest and intra-observer reliability by using the 2-way mixed-effects model (191).

The findings of this study obtained in a small animal model provide a valuable base for continued studies of ventricular volume measurements using ultrasound with clinically adapted frequencies in PT human infants. Potentially, reproducible and accurate ultrasound-based ventricular volume estimation may have important clinical implications. It has been shown recently that larger ventricular volume, determined by MRI at term age, in the human PT infants with IVH was positively correlated to higher global brain abnormality score and negatively correlated to brain growth (11). Moreover, it has been suggested that even light to moderate ventricular dilatation without a preceding IVH in extremely PT infants is predictive of psychiatric disorders at school-age (192,193). It is plausible that the improved discriminatory capacity of 3-D ultrasound measurements can optimize time-points of interventions as well as add predictive power for long-term outcomes.

Paper V

The long-term detrimental effects of IVH and PHVD in a PT rabbit model include alterations of cortical myelination microstructure, altered cortical organization, selectively reduced neuron and pre-synaptic terminal density, and altered PV-positive interneuron number and maturation.

Hypothetical statement

There are little data available on long-term outcomes of the IVH/ PHVD in animal models, limited to term-born animals. The establishment and characterization of the IVH/PHVD model in preterm animals may help to fill the gap in the knowledge.

Findings and discussion

This is the first small animal study reporting data on the long-term effects of IVH and PHVD development in a PT animal model. We observed enduring changes across the cortical structure, neuronal number, synapse density, and myelin structure, but apparently preserved neurobehavioral status.

Unexpectedly, we found reduced survival in female pups, particularly in female pups with IVH. Unfortunately, there is no available data on sex-based survival in short-term studies in PT rabbit pups with IVH. Our data are surprising when compared to the clinical situation where the male sex is still associated with higher mortality and morbidity, including IVH (194). Our data highlight also the importance of reporting and controlling for sex in animal studies.

Data from neurobehavioral assessment in PT rabbit pups with IVH at PND 14 showed impaired locomotion on an inclined surface, gait alteration, and deficient righting reflex (113,142–148). We were unable to detect any differences in these three attributes, which could be explained by the advanced testing time point and maturation *per se* as well as a selection effect due to the survival of healthier animals at PND 30. Similarly, we could not detect any differences in the novel object recognition test, which assesses the memory of the animals. However, the memory task was limited to four hours, which perhaps is too short to detect the differences between the groups. Both the IVH group and control group rabbits exhibited increased anxiety behavior by preferring to remain at the proximity of the wall and this data is in agreement with two other studies performed in PT rabbits (129,138).

The PT pups with IVH/PHVD exhibited reduced myelination in the nucleus caudate, but not in the cortex. The furthered analysis of the organization of MBP stainings demonstrated aberrant myelin fiber organization in PT pups with IVH/PHVD.

Despite the general macroscopic impression of the thinner cortex in IVH/PHVD animals compared to the control group animals (Figure 13), there was no difference in total cortical depth, but it was limited to upper cortical layers (I-III) which were

thinner in IVH/PHVD animals as compared to the controls. Furthermore, IVH/PHVD group animals exhibited a decreased number of PV positive interneurons in the lower cortical layers (IV-VI). The effect of IVH on cortical interneuron population in the PT rabbit pup was assessed for the first time in our study. Such a reduction of cortical PV positive interneurons is in line with data from human PT infants (83). In addition, IVH/PHVD group animals had a lower amount of PV+ PNN- interneurons in all cortical layers, but this was significantly pronounced for the deep cortical layers (IV-VI). To note, tight regulation of the PNN is essential for normal brain function (91).
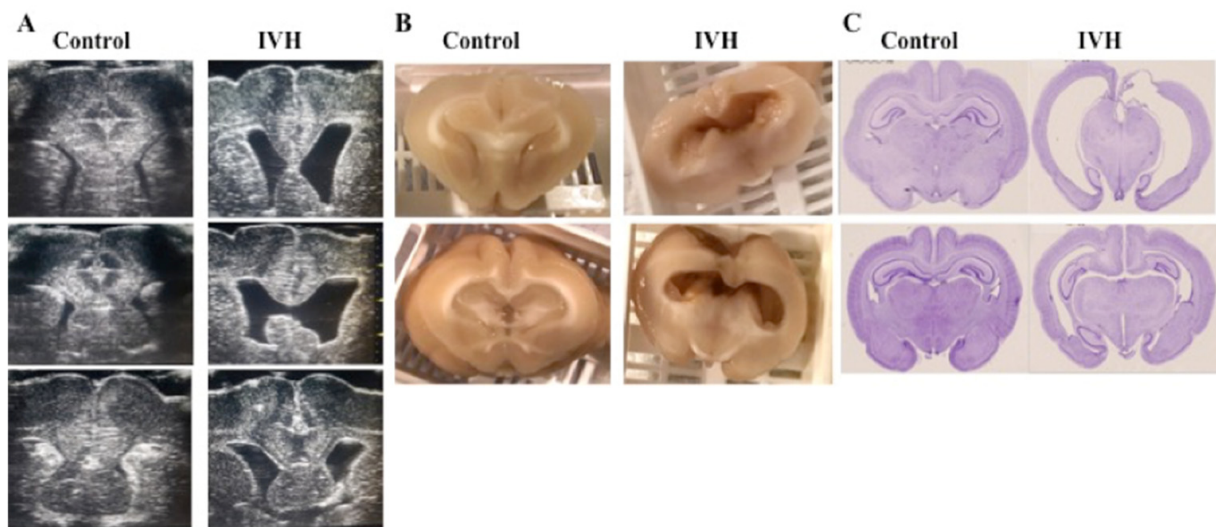
Figure 13. IVH caused a gross disturbance in brain structure. This was visible via (A) HFU *ex vivo* at PND 33 in which coronal sections were obtained in a rostral-caudal direction; (B) at the macroscopic examination; and (C) with HE stains of coronal sections.

Another finding of our study is the decreased expression of synaptophysin in IVH/PHVD group pups, which supports the hypothesis of a disrupted synapse maturation process due to IVH/PHVD in PT rabbit pups.

Furthermore, similarly to human PT infant post-mortem studies (83,153), we found several alterations in brain GM in PT rabbits with IVH/PHVD, characterized by the reduced number of neurons in the nucleus caudate and thalamus, similar to what was observed in other animal models of neonatal brain injury, induced by prematurity, fetal asphyxia and hypoxic-ischemic insult (82,85,195).

Despite the achievement of a long-term IVH/PHVD model in PT rabbit pups, our study has some limitations. One of the major concerns is the high mortality resulting in small sample size and thereby in reduced power for the detection of significant differences between the groups. The "selection effect", characterized by survival of healthiest pups, might obscure possible differences present in the original sample size. This may reflect a better long-term outcome of PT rabbit pups with IVH

compared to that of very sick extremely PT human infants, whose survival is sustained thanks to advanced neonatal intensive care. Moreover, all pups included in the study received glycerol injection resulting in absence of "sham" controls. This hinders the evaluation of the possible adverse effects of glycerol (137). Our neurobehavioral assessment was rather limited and the differences in cognitive assessment could remain undetected at the evaluated time points. More studies are needed to answer these questions and for the furthered understanding of the long-term effects of IVH/PHVD on brain development and consequently neurocognition.

The findings of our study reflect a global injury to the immature brain caused by IVH/PHVD and are fundamental for the furthered understanding of mechanisms leading to WM and GM damage, altered corticogenesis, ultimately causing neurodevelopmental impairment.

Conclusion and future perspectives

Intraventricular hemorrhage is one of the most serious co-morbidities of prematurity with an almost unchanged incidence over the past 15 years. It represents a great challenge for clinicians and researchers due to the lack of effective treatment. Therefore it is important to understand the mechanisms leading to brain damage following IVH, ultimately resulting in adverse neurodevelopment. Thus, the primary focus of this thesis was to provide novel insights into the pathophysiological aspects of IVH/PHVD and its related secondary brain damage that eventually may be used as a base for the development of treatment strategies.

The results of this thesis show that extracellular Hb and its metabolites are important in the pathophysiological cascade that may lead to a long-lasting brain injury following IVH. We found that extracellular Hb was extensively distributed within periventricular white matter following IVH. Therefore targeting extracellular Hb and its metabolites by appropriate scavengers may potentially offer valuable treatment strategies.

Consequently, we investigated whether alpha-1-microglobulin, a free heme and free radical scavenger, might attenuate brain damage following IVH. Firstly, we observed an extensive distribution of intracerebroventricularly administered alpha-1-microglobulin in preterm rabbit pups with IVH. Alpha-1-microglobulin reduced up-regulation of pro-inflammatory markers and the preserved structural integrity of mitochondria in preterm rabbit pups with IVH. These findings suggest that alpha-1-microglobulin may be a possible therapeutic option for IVH. However, several unanswered questions should be addressed to evaluate its effectiveness, safety, and feasibility.

In this thesis we observed a hemorrhage within the subfornicular organ, which is responsible for osmotic homeostasis, suggesting thereby the need for the furthered research to evaluate its possible role in IVH pathogenesis.

We report the data on long-term effects of IVH/PHVD in preterm rabbit pups, namely persistent changes across the cortical structure, myelin, neuronal number, and synapse density. The upper cortical layers (I-III) were thinner in pups with IVH/PHVD. Moreover, we found a reduced number of parvalbumin-positive interneurons and their association with perineural networks in the lower cortical layers (IV-VI) in preterm rabbit pups with IVH. Although there was no detectable

change in total neuronal number in the cortex, we observed reduced neurogenesis in the nucleus caudate. Furthermore, synaptic density and myelin content were reduced in nucleus caudate in preterm rabbit pups with IVH/PHVD. Interestingly, there was no reduction in total cortical myelin content, whereas altered myelin fiber orientation and directionality pattern in IVH/PHVD pups. The findings of this study highlight the deleterious effects of IVH/PHVD on the immature brain, involving both white and gray matter, leading to remodeled corticogenesis. The findings of this study may be one of the first steps in the furthered understanding of mechanisms leading to white and gray matter damage, altered corticogenesis following IVH/PHVD, leaving several unanswered questions that may be addressed in future studies.

In all studies included in this thesis, the presence of IVH was detected by high-frequency ultrasound. In the preterm rabbit pups, IVH evolves rapidly to PHVD. Consequently, we performed the volumetric reconstruction of lateral ventricles by high-frequency ultrasound, which proved to be reproducible, accurate, and reliable as compared to magnetic resonance imaging. However, our study was limited to 48h of life. This clearly indicates the need for longitudinal data including several time-points for estimation of ventricular volume and the evaluation of safety at high frequencies.

The findings of this thesis additionally emphasize the necessity of high-quality systematic reviews in animal studies to assess the benefits and harms of different interventions to highlight research gaps, to avoid unethical research and waste of resources.

Acknowledgments

Professor David Ley

I wish to express my deepest gratitude to my main supervisor, Prof. David Ley, who is a brilliant scientist and a very generous person. You are very patient, humble and open-minded, which makes you a great supervisor. You convincingly guided and encouraged me throughout my PhD project, even when the road was strenuous. Thank you for all the high-level discussions, I´ve learned a lot from them. I am very grateful for all your compliments. They helped me gain my confidence. I am very appreciative of your wise assistance to my growth as a scientist. Importantly, thank you and your wife Eva for welcoming my family and me after we moved to Lund – I will be eternally grateful for your kindness.

Associate Professor Xiaoyang Wang

The wise advice, support and great scientific discussions of my co-supervisor, Ass. Prof. Xiaoyang Wang has been invaluable on both a scientific and a personal level, for which I am profoundly grateful. Your positive attitude and enthusiasm sustained me along my way. I am grateful for all your suggestions and corrections but also compliments. You and David supported substantially my growth as a researcher. Thank you for being a great co-supervisor.

Professor Diana Karpmann

It is a genuine pleasure to express my deep sense of thanks and immense gratitude to my mentor, Prof. Diana Karpmann, who is a top-level scientist and a very kind person. Your words and wise advice encouraged me to find the strength and confidence I needed in the moment of my fragility. I will be always grateful for that, thank you.

Magnus Gram

I owe sincere gratitude to Magnus Gram for his co-operation throughout my PhD studies. Thank you for the great scientific discussions, your kind guidance with meticulous scrutiny on study protocol writing, and your suggestions. You contributed to my scientific growth and I am infinitely grateful for that.

Associate Professor Magnus Cinthio

I very much appreciated working with Ass. Prof. Magnus Cinthio. Thank you for your genuine kindness and respect, for teaching me high-frequency ultrasound machine and some ultrasound basics. It helped me not only as a researcher but also in my clinical activities and I am very appreciative of that. I am grateful for our collaboration projects and your enthusiasm. "Dunder!" was indeed one of the first Swedish words I learned.

Associate Professor Bo Holmqvist

My special thanks are also to Ass. Prof. Bo Holmqvist, who introduced me with enormous patience and meticulous guidance into the immunohistochemistry and immunofluorescence world. Thank you Bo for all the scientific discussions, keen interest, good advice, and suggestions. I appreciate it enormously.

Associate Professor Bobbi Fleiss

I also had the great pleasure of working with Ass. Prof. Bobbi Fleiss who introduced me to cortical layering and interneuron analysis. Thank you Bobbi for great scientific discussions, suggestions, and advice. Although our collaboration started by the end of my PhD project you contributed extensively to my growth as a researcher and I appreciate it very much. Thank you also for your cheerful attitude on our zoom meetings!

My opponent, Associate Professor Cora Nijboer

I wish to express my gratitude to my opponent, Ass. Prof. Cora Nojboer, for taking on the responsibility to assist and to evaluate my dissertation. I will learn from it and it will help my growth as a scientist.

The examination board members

I wish to express my sincere gratitude to examination board members, **Ass. Prof. Sofie Mohlin, Ass. Prof. Karin Tran Lundmark, and Prof. Eric Herlenius**, for assessment of my thesis and evaluation of defense. My thanks go also to the deputy members of the examination board, **Ass. Prof. Valeria Perez de Sa and Ass. Prof. Erik Eklund,** for taking the role of deputy members and for evaluation of my thesis.

Half-time reviewers

I owe thanks also to my half-time reviewers, **Ass. Prof. Pernilla Stenström and Ass. Prof. Erik Eklund**, who took their time to go through my work by the time of the half-time examination. Thank you for being very respectful and for an enormously useful discussion during the examination.

Friends

My dear Friends, no matter where you are, thank you for being always there for me!

Family

Nobody has been more important to me in the pursuit of this project than the members of my lovely family. It is not always easy for me to talk about what is going on, but thanks for being there for me. I know I have the strength to handle anything as long as I have the love of my family behind me. Thank you for always supporting me. I love you. I will be always grateful for each moment we can share.

My parents-in-law, **Laura and Piero**, thank you for your love, care, and respect. Laura, thank you also for all the lovely daughter-in-law dates: despite the years past I still remember our cinema escapes and it makes me smile. Piero, your generosity is admirable and I am grateful to testify it. You are exceptional people and I thank God I met you.

To my brother, **Erlend**, for your love, patience, and support. Thank you for always believing in me no matter what. Thank you for all the cheerful moments. You are a greater treasure than I can imagine.

A very special mention to my lovely parents, **Eila and Wesley**, who gave me all. Thank you for your endless love and respect. Thank you for letting me purchase my dreams and teaching me to believe in myself. My dear mother, although you are not in this world, I know that you are still at my side. My dear father, you are the wisest man I know, thank you for all your advice. I am a very lucky person to have you as my parents!

Marco and Luca, you are the best gift I could ever have. You fill every day with love and joy, warmth and kindness. Thank you! Follow your dreams, because everything is possible. I love you and I believe in you!

Finally, a special "thank you" to my dear husband **Matteo** for being there for me:

> "You are my North, my South, my East and West,
>
> My working week and my Sunday rest,
>
> My noon, my midnight, my talk, my song!" *(modified from W.H. Auden)*

Thank you, Matteo!

References

1. Stoll BJ, Hansen NI, Bell EF, Walsh MC, Carlo WA, Shankaran S, et al. Trends in care practices, morbidity, and mortality of extremely preterm neonates, 1993-2012. JAMA. 2015;314(10):1039.

2. Ahn SY, Shim S-Y, Sung IK. Intraventricular hemorrhage and post hemorrhagic hydrocephalus among very-low-birth-weight infants in Korea. J Korean Med Sci. 2015;30 Suppl 1:S52-58.

3. Ishii N, Kono Y, Yonemoto N, Kusuda S, Fujimura M, for the Neonatal Research Network, Japan. Outcomes of infants born at 22 and 23 weeks' gestation. Pediatrics. 2013;132(1):62–71.

4. Garfinkle J, Yoon EW, Alvaro R, Nwaesei C, Claveau M, Lee SK, et al. Trends in sex-specific differences in outcomes in extreme preterms: progress or natural barriers? Arch Dis Child Fetal Neonatal Ed. 2020;105(2):158–63.

5. Szpecht D, Nowak I, Kwiatkowska P, Szymankiewicz M, Gadzinowski J. Intraventricular hemorrhage in neonates born from 23 to 26 weeks of gestation: retrospective analysis of risk factors. Adv Clin Exp Med. 2017;26(1):89–94.

6. Yeo KT, Thomas R, Chow SS, Bolisetty S, Haslam R, Tarnow-Mordi W, et al. Improving incidence trends of severe intraventricular haemorrhages in preterm infants <32 weeks gestation: a cohort study. Arch Dis Child Fetal Neonatal Ed. 2020;105(2):145–50.

7. Brouwer A, Groenendaal F, Haastert I-L van, Rademaker K, Hanlo P, Vries L de. Neurodevelopmental outcome of preterm infants with severe intraventricular hemorrhage and therapy for post-hemorrhagic ventricular dilatation. J Pediatr. 2008;152(5):648–54.

8. Whitelaw A, Evans D, Carter M, Thoresen M, Wroblewska J, Mandera M, et al. Randomized clinical trial of prevention of hydrocephalus after intraventricular hemorrhage in preterm infants: brain-washing versus tapping fluid. Pediatrics. 2007;119(5):e1071–8.

9. Adams-Chapman I, Hansen NI, Stoll BJ, Higgins R, NICHD Research Network. Neurodevelopmental outcome of extremely low birth weight infants with posthemorrhagic hydrocephalus requiring shunt insertion. Pediatrics. 2008;121(5):e1167-1177.

10. Bassan H, Eshel R, Golan I, Kohelet D, Ben Sira L, Mandel D, et al. Timing of external ventricular drainage and neurodevelopmental outcome in preterm infants with posthemorrhagic hydrocephalus. Eur J Paediatr Neurol. 2012;16(6):662–70.

11. Cizmeci MN, Khalili N, Claessens NH, Groenendaal F, Liem KD, Heep A, et al. Assessment of brain injury and brain volumes after posthemorrhagic ventricular

dilatation: a nested substudy of the randomized controlled ELVIS trial. J Pediatr. 2019;208:191-197.e2.

12. Luyt K, Jary SL, Lea CL, Young GJ, Odd DE, Miller HE, et al. Drainage, irrigation and fibrinolytic therapy (DRIFT) for posthaemorrhagic ventricular dilatation: 10-year follow-up of a randomised controlled trial. Arch Dis Child Fetal Neonatal Ed. 2020;105(5):466–73.

13. Shankaran S, Bajaj M, Natarajan G, Saha S, Pappas A, Davis AS, et al. Outcomes following post-hemorrhagic ventricular dilatation among infants of extremely low gestational age. J Pediatr. 2020;226:36-44.e3.

14. Gould SJ, Howard S. An immunohistochemical study of the germinal layer in the late gestation human fetal brain. Neuropathol Appl Neurobiol. 1987;13(6):421–37.

15. Ballabh P. Pathogenesis and prevention of intraventricular hemorrhage. Clin Perinatol. 2014;41(1):47–67.

16. Ballabh P, Xu H, Hu F, Braun A, Smith K, Rivera A, et al. Angiogenic inhibition reduces germinal matrix hemorrhage. Nat Med. 2007;13(4):9.

17. Goddard J, Lewis RM, Armstrong DL, Zeller RS. Moderate, rapidly induced hypertension as a cause of intraventricular hemorrhage in the newborn beagle model. J Pediatr. 1980;96(6):1057–60.

18. Ment LR, Stewart WB, Duncan CC, Lambrecht R. Beagle puppy model of intraventricular hemorrhage. J Neurosurg. 1982;57(2):219–23.

19. Pasternak JF, Groothuis DR, Fischer JM, Fischer DP. Regional cerebral blood flow in the beagle puppy model of neonatal intraventricular hemorrhage: studies during systemic hypertension. Neurology. 1983;33(5):559–66.

20. Nagano N, Saito M, Sugiura T, Miyahara F, Namba F, Ota E. Benefits of umbilical cord milking versus delayed cord clamping on neonatal outcomes in preterm infants: A systematic review and meta-analysis. PloS One. 2018;13(8):e0201528.

21. Dudink J, Jeanne Steggerda S, Horsch S, eurUS.brain group. State-of-the-art neonatal cerebral ultrasound: technique and reporting. Pediatr Res. 2020;87(Suppl 1):3–12.

22. Papile LA, Burstein J, Burstein R, Koffler H. Incidence and evolution of subependymal and intraventricular hemorrhage: A study of infants with birth weights less than 1,500 gm. J Pediatr. 1978;92(4):529–34.

23. Volpe J. Neurology of the Newborn. 5th ed. Philadeplphia: Saunders, Elsivier; 2008. pp. 517-588.

24. Mukerji A, Shah V, Shah PS. Periventricular/Intraventricular hemorrhage and neurodevelopmental outcomes: A meta-analysis. Pediatrics. 2015;136(6):1132–43.

25. Kim JK, Chang YS, Sung S, Park WS. Mortality rate-dependent variations in the survival without major morbidities rate of extremely preterm infants. Sci Rep. 2019;9(1):7371.

26. Parodi A, Govaert P, Horsch S, Bravo MC, Ramenghi LA, eurUS.brain group. Cranial ultrasound findings in preterm germinal matrix haemorrhage, sequelae and outcome. Pediatr Res. 2020;87(Suppl 1):13–24.

27. Badhiwala JH, Hong CJ, Nassiri F, Hong BY, Riva-Cambrin J, Kulkarni AV. Treatment of posthemorrhagic ventricular dilation in preterm infants: a systematic

review and meta-analysis of outcomes and complications. J Neurosurg Pediatr. 2015;16(5):545–55.

28. Leijser LM, Miller SP, van Wezel-Meijler G, Brouwer AJ, Traubici J, van Haastert IC, et al. Posthemorrhagic ventricular dilatation in preterm infants:When best to intervene? Neurology. 2018;90(8):e698–706.

29. Davies MW. Reference ranges for the linear dimensions of the intracranial ventricles in preterm neonates. Arch Dis Child - Fetal Neonatal Ed. 2000 May 1;82(3):218F – 223.

30. Dorner RA, Burton VJ, Allen MC, Robinson S, Soares BP. Preterm neuroimaging and neurodevelopmental outcome: a focus on intraventricular hemorrhage, post-hemorrhagic hydrocephalus, and associated brain injury. J Perinatol. 2018;38(11):1431–43.

31. Olischar M, Klebermass K, Hengl B, Hunt RW, Waldhoer T, Pollak A, et al. Cerebrospinal fluid drainage in posthaemorrhagic ventricular dilatation leads to improvement in amplitude-integrated electroencephalographic activity. Acta Paediatr. 2009;98(6):1002–9.

32. Klebermass-Schrehof K, Rona Z, Waldhör T, Czaba C, Beke A, Weninger M, et al. Can neurophysiological assessment improve timing of intervention in posthaemorrhagic ventricular dilatation? Arch Dis Child Fetal Neonatal Ed. 2013;98(4):F291–7.

33. Aquilina K, Chakkarapani E, Thoresen M. Early deterioration of cerebrospinal fluid dynamics in a neonatal piglet model of intraventricular hemorrhage and posthemorrhagic ventricular dilation: Laboratory investigation. J Neurosurg Pediatr. 2012;10(6):529–37.

34. Karimy JK, Zhang J, Kurland DB, Theriault BC, Duran D, Stokum JA, et al. Inflammation-dependent cerebrospinal fluid hypersecretion by the choroid plexus epithelium in posthemorrhagic hydrocephalus. Nat Med. 2017;23(8):10.

35. Romantsik O, Bruschettini M, Ley D. Intraventricular hemorrhage and white matter injury in preclinical and clinical studies. NeoReviews. 2019;20(11):e636–52.

36. Papadopoulos MC, Verkman AS. Aquaporin water channels in the nervous system. Nat Rev Neurosci. 2013;14(4):265–77.

37. Oshio K, Watanabe H, Song Y, Verkman AS, Manley GT. Reduced cerebrospinal fluid production and intracranial pressure in mice lacking choroid plexus water channel Aquaporin-1. FASEB J. 2005;19(1):76–8.

38. Sveinsdottir S, Gram M, Cinthio M, Sveinsdottir K, Mörgelin M, Ley D. Altered expression of aquaporin 1 and 5 in the choroid plexus following preterm intraventricular hemorrhage. Dev Neurosci. 2014;36(6):542–51.

39. Whitelaw A, Jary S, Kmita G, Wroblewska J, Musialik-Swietlinska E, Mandera M, et al. Randomized trial of drainage, irrigation and fibrinolytic therapy for premature infants with posthemorrhagic ventricular dilatation: developmental outcome at 2 years. Pediatrics. 2010;125(4):e852–8.

40. Lee KR, Colon GP, Betz AL, Keep RF, Kim S, Hoff JT. Edema from intracerebral hemorrhage: the role of thrombin. J Neurosurg. 1996;84(1):91–6.

41. Vaughan P, Pike C, Cotman C, Cunningham D. Thrombin receptor activation protects neurons and astrocytes from cell death produced by environmental insults. J Neurosci. 1995;15(7):5389–401.

42. Masada T, Xi G, Hua Y, Keep RF. The effects of thrombin preconditioning on focal cerebral ischemia in rats. Brain Res. 2000;867(1–2):173–9.

43. Xi G, Reiser G, Keep RF. The role of thrombin and thrombin receptors in ischemic, hemorrhagic and traumatic brain injury: deleterious or protective? Thrombin and thrombin receptors in brain injury. J Neurochem. 2002;84(1):3–9.

44. Jiang Y, Wu J, Hua Y, Keep RF, Xiang J, Hoff JT, et al. Thrombin-receptor activation and thrombin-induced brain tolerance. J Cereb Blood Flow Metab. 2002;22(4):404–10.

45. Coughlin SR. Thrombin signalling and protease-activated receptors. Nature. 2000;407(6801):258–64.

46. Gao F, Liu F, Chen Z, Hua Y, Keep RF, Xi G. Hydrocephalus after intraventricular hemorrhage: the role of thrombin. J Cereb Blood Flow Metab. 2014;34(3):489–94.

47. Chang JJ, Emanuel BA, Mack WJ, Tsivgoulis G, Alexandrov AV. Matrix metalloproteinase-9: dual role and temporal profile in intracerebral hemorrhage. J Stroke Cerebrovasc Dis Off J Natl Stroke Assoc. 2014;23(10):2498–505.

48. Zhang X, Gu Y, Li P, Jiang A, Sheng X, Jin X, et al. Matrix metalloproteases-mediated cleavage on β-dystroglycan may play a key role in the blood–brain barrier after intracerebral hemorrhage in rats. Med Sci Monit. 2019;25:794–800.

49. Liu D-Z, Ander BP, Xu H, Shen Y, Kaur P, Deng W, et al. Blood-brain barrier breakdown and repair by Src after thrombin-induced injury. Ann Neurol. 2010;67(4):526–33.

50. Davalos D, Kyu Ryu J, Merlini M, Baeten KM, Le Moan N, Petersen MA, et al. Fibrinogen-induced perivascular microglial clustering is required for the development of axonal damage in neuroinflammation. Nat Commun. 2012;3(1):1227.

51. Whitelaw A, Christie S, Pople I. Transforming growth factor-beta 1: a possible signal molecule for posthemorrhagic hydrocephalus? Pediatr Res. 1999;46(5):576–80.

52. Botfield H, Gonzalez AM, Abdullah O, Skjolding AD, Berry M, McAllister JP, et al. Decorin prevents the development of juvenile communicating hydrocephalus. Brain. 2013;136(9):2842–58.

53. Aojula A, Botfield H, McAllister JP, Gonzalez AM, Abdullah O, Logan A, et al. Diffusion tensor imaging with direct cytopathological validation: characterisation of decorin treatment in experimental juvenile communicating hydrocephalus. Fluids Barriers CNS. 2016;13(1):9.

54. Yao C-S, Yan S-G, Gao L-S, Sun Z-R, Liu F, Jiang B, et al. Patients with risk factors have higher plasma levels of lysophosphatidic acid: a promising surrogate marker for blood platelet activation. Blood Coagul Fibrinolysis Int J Haemost Thromb. 2014;25(4):322–5.

55. Park R, Moon UY, Park JY, Hughes LJ, Johnson RL, Cho S-H, et al. Yap is required for ependymal integrity and is suppressed in LPA-induced hydrocephalus. Nat Commun. 2016;7(1):10329.

56. Gram M, Sveinsdottir S, Ruscher K, Hansson SR, Cinthio M, Åkerström B, et al. Hemoglobin induces inflammation after preterm intraventricular hemorrhage by methemoglobin formation. J Neuroinflammation. 2013;10(1):867.

57. Reeder BJ. The redox activity of hemoglobins: from physiologic functions to pathologic mechanisms. Antioxid Redox Signal. 2010;13(7):1087–123.

58. Olsson MG, Allhorn M, Bülow L, Hansson SR, Ley D, Olsson ML, et al. Pathological conditions involving extracellular hemoglobin: molecular mechanisms, clinical significance, and novel therapeutic opportunities for α_1 -microglobulin. Antioxid Redox Signal. 2012;17(5):813–46.

59. Umbreit J. Methemoglobin—it's not just blue: A concise review. Am J Hematol. 2007;82(2):134–44.

60. Kumar S, Bandyopadhyay U. Free heme toxicity and its detoxification systems in human. Toxicol Lett. 2005;157(3):175–88.

61. Belcher JD, Beckman JD, Balla G, Balla J, Vercellotti G. Heme degradation and vascular injury. Antioxid Redox Signal. 2010;12(2):233–48.

62. Gram M, Sveinsdottir S, Cinthio M, Sveinsdottir K, Hansson SR, Mörgelin M, et al. Extracellular hemoglobin-mediator of inflammation and cell death in the choroid plexus following preterm intraventricular hemorrhage. J Neuroinflammation. 2014;11(1):200.

63. Kaur C, Ling EA. Periventricular white matter damage in the hypoxic neonatal brain: Role of microglial cells. Prog Neurobiol. 2009;87(4):264–80.

64. deLuca LS, Gommerman JL. Fine-tuning of dendritic cell biology by the TNF superfamily. Nat Rev Immunol. 2012;12(5):339–51.

65. Massicotte EM, Del Bigio MR. Human arachnoid villi response to subarachnoid hemorrhage: possible relationship to chronic hydrocephalus. J Neurosurg. 1999;91(1):80–4.

66. Chen Z, Gao C, Hua Y, Keep RF, Muraszko K, Xi G. Role of iron in brain injury after intraventricular hemorrhage. Stroke. 2011;42(2):465–70.

67. Savman K, Nilsson UA, Blennow M, Kjellmer I, Whitelaw A. Non-protein-bound iron is elevated in cerebrospinal fluid from preterm infants with posthemorrhagic ventricular dilatation. Pediatr Res. 2001;49(2):208–12.

68. Back SA, Luo NL, Mallinson RA, O'Malley JP, Wallen LD, Frei B, et al. Selective vulnerability of preterm white matter to oxidative damage defined by F2-isoprostanes. Ann Neurol. 2005;58(1):108–20.

69. Khwaja O, Volpe JJ. Pathogenesis of cerebral white matter injury of prematurity. Arch Dis Child Fetal Neonatal Ed. 2007;93(2):F153–61.

70. Mullen KM, Vohr BR, Katz KH, Schneider KC, Lacadie C, Hampson M, et al. Preterm birth results in alterations in neural connectivity at age 16 years. NeuroImage. 2011;54(4):2563–70.

71. Ball G, Boardman JP, Aljabar P, Pandit A, Arichi T, Merchant N, et al. The influence of preterm birth on the developing thalamocortical connectome. Cortex. 2013;49(6):1711–21.

72. Ball G, Pazderova L, Chew A, Tusor N, Merchant N, Arichi T, et al. Thalamocortical connectivity predicts cognition in children born preterm. Cereb Cortex. 2015;25(11):4310–8.

73. Fukumizu M, Takashima S, Becker LE. Neonatal posthemorrhagic hydrocephalus: neuropathologic and immunohistochemical studies. Pediatr Neurol. 1995;13(3):230–4.

74. Koeppen AH, Michael SC, Li D, Chen Z, Cusack MJ, Gibson WM, et al. The pathology of superficial siderosis of the central nervous system. Acta Neuropathol (Berl). 2008;116(4):371–82.

75. Agyemang AA, Sveinsdóttir K, Vallius S, Sveinsdóttir S, Bruschettini M, Romantsik O, et al. Cerebellar exposure to cell-free hemoglobin following preterm intraventricular hemorrhage: causal in cerebellar damage? Transl Stroke Res. 2017;8(5):461–73.

76. Loane DJ, Kumar A, Stoica BA, Cabatbat R, Faden AI. Progressive neurodegeneration after experimental brain trauma: Association with chronic microglial activation. J Neuropathol Exp Neurol. 2014;73(1):16.

77. Rathbone R, Counsell SJ, Kapellou O, Dyet L, Kennea N, Hajnal J, et al. Perinatal cortical growth and childhood neurocognitive abilities. Neurology. 2011;77(16):1510–7.

78. Fleiss B, Gressens P, Stolp HB. Cortical gray matter injury in encephalopathy of prematurity: link to neurodevelopmental disorders. Front Neurol. 2020;11:575.

79. Bora S, Pritchard VE, Chen Z, Inder TE, Woodward LJ. Neonatal cerebral morphometry and later risk of persistent inattention/hyperactivity in children born very preterm. J Child Psychol Psychiatry. 2014;55(7):828–38.

80. Bjuland KJ, Rimol LM, Løhaugen GCC, Skranes J. Brain volumes and cognitive function in very-low-birth-weight (VLBW) young adults. Eur J Paediatr Neurol. 2014;18(5):578–90.

81. Zhang Y, Inder TE, Neil JJ, Dierker DL, Alexopoulos D, Anderson PJ, et al. Cortical structural abnormalities in very preterm children at 7 years of age. NeuroImage. 2015;109:469–79.

82. Dieni S, Inder T, Yoder B, Briscoe T, Camm E, Egan G, et al. The pattern of cerebral injury in a primate model of preterm birth and neonatal intensive care. J Neuropathol Exp Neurol. 2004;63(12):1297–309.

83. Panda S, Dohare P, Jain S, Parikh N, Singla P, Mehdizadeh R, et al. Estrogen treatment reverses prematurity-induced disruption in cortical interneuron population. J Neurosci. 2018;38(34):7378–91.

84. Stolp HB, Fleiss B, Arai Y, Supramaniam V, Vontell R, Birtles S, et al. Interneuron development is disrupted in preterm brains with diffuse white matter injury: Observations in mouse and human. Front Physiol. 2019;10:955.

85. McClendon E, Chen K, Gong X, Sharifnia E, Hagen M, Cai V, et al. Prenatal cerebral ischemia triggers dysmaturation of caudate projection neurons. Ann Neurol. 2015;75(4):508–24.

86. McClendon E, Wang K, Degener-O'Brien K, Hagen MW, Gong X, Nguyen T, et al. Transient hypoxemia disrupts anatomical and functional maturation of preterm fetal ovine CA1 pyramidal neurons. J Neurosci. 2019;39(40):7853–71.

87. Fowke TM, Galinsky R, Davidson JO, Wassink G, Karunasinghe RN, Prasad JD, et al. Loss of interneurons and disruption of perineuronal nets in the cerebral cortex following hypoxia-ischaemia in near-term fetal sheep. Sci Rep. 2018;8(1):17686.

88. Lim L, Mi D, Llorca A, Marín O. Development and functional diversification of cortical interneurons. Neuron. 2018;100(2):294–313.

89. Ruden JB, Dugan LL, Konradi C. Parvalbumin interneuron vulnerability and brain disorders. Neuropsychopharmacology. 2021;46(2):279–87.

90. Vaes JEG, Kosmeijer CM, Kaal M, van Vliet R, Brandt MJV, Benders MJNL, et al. Regenerative therapies to restore interneuron disturbances in experimental models of encephalopathy of prematurity. Int J Mol Sci. 2020;22(1):211.

91. Lorenzo Bozzelli P, Alaiyed S, Kim E, Villapol S, Conant K. Proteolytic remodeling of perineuronal nets: Effects on synaptic plasticity and neuronal population dynamics. Neural Plast. 2018;2018:1–13.

92. Sugiyama S, Di Nardo AA, Aizawa S, Matsuo I, Volovitch M, Prochiantz A, et al. Experience-dependent transfer of Otx2 homeoprotein into the visual cortex activates postnatal plasticity. Cell. 2008;134(3):508–20.

93. Bernard C, Prochiantz A. Otx2-PNN interaction to regulate cortical plasticity. Neural Plast. 2016;2016:1–7.

94. Planques A, Oliveira Moreira V, Dubreuil C, Prochiantz A, Di Nardo AA. OTX2 signals from the choroid plexus to regulate adult neurogenesis. eNeuro. 2019;6(2):ENEURO.0262-18.2019.

95. Lee HHC, Bernard C, Ye Z, Acampora D, Simeone A, Prochiantz A, et al. Genetic Otx2 mis-localization delays critical period plasticity across brain regions. Mol Psychiatry. 2017;22(5):680–8.

96. Wen TH, Binder DK, Ethell IM, Razak KA. The perineuronal 'safety' net? Perineuronal net abnormalities in neurological disorders. Front Mol Neurosci. 2018;11:270.

97. Smeds E, Romantsik O, Jungner Å, Erlandsson L, Gram M. Pathophysiology of extracellular haemoglobin: use of animal models to translate molecular mechanisms into clinical significance. ISBT Sci Ser. 2017;12(1):134–41.

98. Allhorn M, Klapyta A, Åkerström B. Redox properties of the lipocalin α1-microglobulin: Reduction of cytochrome c, hemoglobin, and free iron. Free Radic Biol Med. 2005;38(5):557–67.

99. Åkerström B, Gram M. A1M, an extravascular tissue cleaning and housekeeping protein. Free Radic Biol Med. 2014;74:274–82.

100. Olsson MG, Rosenlöf LW, Kotarsky H, Olofsson T, Leanderson T, Mörgelin M, et al. The radical-binding lipocalin A1M binds to a complex I subunit and protects mitochondrial structure and function. Antioxid Redox Signal. 2013;18(16):2017–28.

101. Takagi K, Kin K, Itoh Y, Enomoto H, Kawai T. Human alpha 1-microglobulin levels in various body fluids. J Clin Pathol. 1980;33(8):786–91.

102. Itoh Y, Enomoto H, Takagi K, Obayashi T, Kawai T. Human alpha 1-microglobulin levels in neurological disorders. Eur Neurol. 1983;22(1):1–6.

103. Kwasek A, Osmark P, Allhorn M, Lindqvist A, Åkerström B, Wasylewski Z. Production of recombinant human α1-microglobulin and mutant forms involved in chromophore formation. Protein Expr Purif. 2007;53(1):145–52.

104. Åkerström B, Rosenlöf L, Hägerwall A, Rutardottir S, Ahlstedt J, Johansson ME, et al. rA1M-035, a physicochemically improved human recombinant α $_1$ -microglobulin, has therapeutic effects in rhabdomyolysis-induced acute kidney injury. Antioxid Redox Signal. 2019;30(4):489–504.

105. Aquilina K, Chakkarapani E, Love S, Thoresen M. Neonatal rat model of intraventricular haemorrhage and post-haemorrhagic ventricular dilatation with long-term survival into adulthood: Neonatal rat model of intraventricular haemorrhage surviving into adulthood. Neuropathol Appl Neurobiol. 2011;37(2):156–65.

106. Aquilina K, Hobbs C, Cherian S, Tucker A, Porter H, Whitelaw A, et al. A neonatal piglet model of intraventricular hemorrhage and posthemorrhagic ventricular dilation. J Neurosurg Pediatr. 2007;107(2):126–36.

107. Strahle JM, Garton T, Bazzi AA, Kilaru H, Garton HJL, Maher CO, et al. Role of hemoglobin and iron in hydrocephalus after neonatal intraventricular hemorrhage. Neurosurgery. 2014;75(6):696–706.

108. Garton TP, He Y, Garton HJL, Keep RF, Xi G, Strahle JM. Hemoglobin-induced neuronal degeneration in the hippocampus after neonatal intraventricular hemorrhage. Brain Res. 2016;1635:86–94.

109. Zhu W, Gao Y, Chang C-F, Wan J, Zhu S, Wang J. Mouse models of intracerebral hemorrhage in ventricle, cortex, and hippocampus by injections of autologous blood or collagenase. Ahmad M, editor. PloS One. 2014;9(5):e97423.

110. MacLellan CL, Silasi G, Poon CC, Edmundson CL, Buist R, Peeling J, et al. Intracerebral hemorrhage models in rat: comparing collagenase to blood infusion. J Cereb Blood Flow Metab. 2008;28(3):516–25.

111. Alles YCJ, Greggio S, Alles RM, Azevedo PN, Xavier LL, DaCosta JC. A novel preclinical rodent model of collagenase-induced germinal matrix/intraventricular hemorrhage. Brain Res. 2010;1356:130–8.

112. Tomita H, Ito U, Ohno K, Hirakawa K. Chronological changes in brain edema induced by experimental intracerebral hematoma in cats. Acta Neurochir Suppl (Wien). 1994;60:558–60.

113. Chua CO, Chahboune H, Braun A, Dummula K, Chua CE, Yu J, et al. Consequences of intraventricular hemorrhage in a rabbit pup model. Stroke. 2009;40(10):3369–77.

114. Sveinsdottir S, Cinthio M, Ley D. High-Frequency Ultrasound in the Evaluation of Cerebral Intraventricular Haemorrhage in Preterm Rabbit Pups. Ultrasound Med Biol. 2012 Mar;38(3):423–31.

115. Semple BD, Blomgren K, Gimlin K, Ferriero DM, Noble-Haeusslein LJ. Brain development in rodents and humans: Identifying benchmarks of maturation and vulnerability to injury across species. Prog Neurobiol. 2013;106–107:1–16.

116. Salaets T, Aertgeerts M, Gie A, Vignero J, de Winter D, Regin Y, et al. Preterm birth impairs postnatal lung development in the neonatal rabbit model. Respir Res. 2020;21(1):59.

117. Bozeman AP, Dassinger MS, Birusingh RJ, Burford JM, Smith SD. An animal model of necrotizing enterocolitis (NEC) in preterm rabbits. Fetal Pediatr Pathol. 2013;32(2):113–22.

118. de Winter D, Salaets T, Gie A, Deprest J, Levtchenko E, Toelen J. Glomerular developmental delay and proteinuria in the preterm neonatal rabbit. Simeoni U, editor. PloS One. 2020;15(11):e0241384.

119. Sveinsdóttir K, Länsberg J-K, Sveinsdóttir S, Garwicz M, Ohlsson L, Hellström A, et al. Impaired cerebellar maturation, growth restriction, and circulating insulin-like growth factor 1 in preterm rabbit pups. Dev Neurosci. 2017;39(6):487–97.

120. Georgiadis P, Xu H, Chua C, Hu F, Collins L, Huynh C, et al. Characterization of acute brain injuries and neurobehavioral profiles in a rabbit model of germinal matrix hemorrhage. Stroke. 2008;39(12):3378–88.

121. Lorenzo AV, Welch K, Conner S. Spontaneous germinal matrix and intraventricular hemorrhage in prematurely born rabbits. J Neurosurg. 1982;56(3):404–10.

122. Conner ES, Lorenzo AV, Welch K, Dorval B. The role of intracranial hypotension in neonatal intraventricular hemorrhage. J Neurosurg. 1983;58(2):204–9.

123. Harel S, Watanabe K, Linke I, Schain RJ. Growth and development of the rabbit brain. Neonatology. 1972;21(5–6):381–99.

124. Derrick M, Drobyshevsky A, Ji X, Tan S. A model of cerebral palsy from fetal hypoxia-ischemia. Stroke. 2007;38(2):731–5.

125. Ferraris S, van der Merwe J, Van Der Veeken L, Prados F, Iglesias J-E, Melbourne A, et al. A magnetic resonance multi-atlas for the neonatal rabbit brain. NeuroImage. 2018;179:187–98.

126. Drobyshevsky A, Jiang R, Derrick M, Luo K, Tan S. Functional correlates of central white matter maturation in perinatal period in rabbits. Exp Neurol. 2014;261:76–86.

127. Lekic T, Manaenko A, Rolland W, Tang J, Zhang JH. A novel preclinical model of germinal matrix hemorrhage using neonatal rats. In: Intracerebral Hemorrhage Research. Vienna: Springer Vienna; 2011. p. 55–60. (Acta Neurochirurgica Supplementum; vol. 111).

128. Illa M, Eixarch E, Batalle D, Arbat-Plana A, Muñoz-Moreno E, Figueras F, et al. Long-term functional outcomes and correlation with regional brain connectivity by MRI diffusion tractography metrics in a near-term rabbit model of intrauterine growth restriction. PloS One. 2013;8(10):e76453.

129. Klebe D, Tibrewal M, Sharma DR, Vanaparthy R, Krishna S, Varghese M, et al. Reduced hippocampal dendrite branching, spine density and neurocognitive function in premature rabbits, and reversal with estrogen or TrkB agonist treatment. Cereb Cortex. 2019;29(12):4932–47.

130. Schaal B, Coureaud G, Langlois D, Giniès C, Sémon E, Perrier G. Chemical and behavioural characterization of the rabbit mammary pheromone. Nature. 2003;424(6944):68–72.

131. Montigny D, Coureaud G, Schaal B. Rabbit pup response to the mammary pheromone: From automatism to prandial control. Physiol Behav. 2006;89(5):742–9.

132. Charra R, Datiche F, Gigot V, Schaal B, Coureaud G. Pheromone-induced odor learning modifies Fos expression in the newborn rabbit brain. Behav Brain Res. 2013;237:129–40.

133. Schneider NY, Piccin C, Datiche F, Coureaud G. Spontaneous brain processing of the mammary pheromone in rabbit neonates prior to milk intake. Behav Brain Res. 2016;313:191–200.

134. Schaal B, Coureaud G, Doucet S, Delaunay-El Allam M, Moncomble A-S, Montigny D, et al. Mammary olfactory signalisation in females and odor processing in neonates: Ways evolved by rabbits and humans. Behav Brain Res. 2009;200(2):346–58.

135. Ecury-Goossen GM, Camfferman FA, Leijser LM, Govaert P, Dudink J. State of the art cranial ultrasound imaging in neonates. J Vis Exp. 2015;(96):52238.

136. Fischer B, Chavatte-Palmer P, Viebahn C, Navarrete Santos A, Duranthon V. Rabbit as a reproductive model for human health. Reproduction. 2012;144(1):1–10.

137. Traudt CM, McPherson RJ, Studholme C, Millen KJ, Juul SE. Systemic glycerol decreases neonatal rabbit brain and cerebellar growth independent of intraventricular hemorrhage. Pediatr Res. 2014;75(3):389–94.

138. Van der Veeken L, Grönlund S, Gerdtsson E, Holmqvist B, Deprest J, Ley D, et al. Long-term neurological effects of neonatal caffeine treatment in a rabbit model of preterm birth. Pediatr Res. 2020;87(6):1011–8.

139. Ang ESBC, Gluncic V, Duque A, Schafer ME, Rakic P. Prenatal exposure to ultrasound waves impacts neuronal migration in mice. Proc Natl Acad Sci. 2006;103(34):12903–10.

140. Maršál K. Exposure to ultrasound in utero: epidemiology and relevance of neuronal migration studies. Ultrasound Med Biol. 2010;36(8):1221–3.

141. Larsson J, Wingårdh K, Berggård T, Davies JR, Lögdberg L, Strand S-E, et al. Distribution of iodine 125–labeled α1-microglobulin in rats after intravenous injection. J Lab Clin Med. 2001;137(3):165–75.

142. Vose LR, Vinukonda G, Jo S, Miry O, Diamond D, Korumilli R, et al. Treatment with thyroxine restores myelination and clinical recovery after intraventricular hemorrhage. J Neurosci. 2013;33(44):17232–46.

143. Vinukonda G, Dohare P, Arshad A, Zia MT, Panda S, Korumilli R, et al. Hyaluronidase and hyaluronan oligosaccharides promote neurological recovery after intraventricular hemorrhage. J Neurosci. 2016;36(3):872–89.

144. Vinukonda G, Zia MT, Bhimavarapu BBR, Hu F, Feinberg M, Bokhari A, et al. Intraventricular hemorrhage induces deposition of proteoglycans in premature rabbits, but their in vivo degradation with chondroitinase does not restore myelination, ventricle size and neurological recovery. Exp Neurol. 2013;247:630–44.

145. Vinukonda G, Liao Y, Hu F, Ivanova L, Purohit D, Finkel DA, et al. Human cord blood-derived unrestricted somatic stem cell infusion improves neurobehavioral outcome in a rabbit model of intraventricular hemorrhage. STEM CELLS Transl Med. 2019;8(11):1157–69.

146. Dohare P, Zia MT, Ahmed E, Ahmed A, Yadala V, Schober AL, et al. AMPA-kainate receptor inhibition promotes neurologic recovery in premature rabbits with intraventricular hemorrhage. J Neurosci. 2016;36(11):3363–77.

147. Dohare P, Cheng B, Ahmed E, Yadala V, Singla P, Thomas S, et al. Glycogen synthase kinase-3β inhibition enhances myelination in preterm newborns with intraventricular hemorrhage, but not recombinant Wnt3A. Neurobiol Dis. 2018;118:22–39.

148. Dohare P, Kidwai A, Kaur J, Singla P, Krishna S, Klebe D, et al. GSK3β inhibition restores impaired neurogenesis in preterm neonates with intraventricular hemorrhage. Cereb Cortex. 2019;29(8):3482–95.

149. Gümüş HG, Agyemang AA, Romantsik O, Sandgren R, Karlsson H, Gram M, et al. Behavioral testing and litter effects in the rabbit. Behav Brain Res. 2018;353:236–41.

150. McFadden WC, Walsh H, Richter F, Soudant C, Bryce CH, Hof PR, et al. Perfusion fixation in brain banking: a systematic review. Acta Neuropathol Commun. 2019;7(1):146.

151. Plum F. Atlas of the rabbit brain and spinal cord. By Shek JW, Wen GY, Wisniewski HM. New York, Karger, 1986. Ann Neurol. 1987;

152. Dummula K, Vinukonda G, Chu P, Xing Y, Hu F, Mailk S, et al. Bone morphogenetic protein inhibition promotes neurological recovery after intraventricular hemorrhage. J Neurosci. 2011;31(34):12068–82.

153. Vontell R, Supramaniam V, Wyatt-Ashmead J, Gressens P, Rutherford M, Hagberg H, et al. Cellular mechanisms of Toll-like receptor-3 activation in the thalamus are associated with white matter injury in the developing brain. J Neuropathol Exp Neurol. 2015;74(3):13.

154. van Tilborg E, van Kammen CM, de Theije CGM, van Meer MPA, Dijkhuizen RM, Nijboer CH. A quantitative method for microstructural analysis of myelinated axons in the injured rodent brain. Sci Rep. 2017;7(1):16492.

155. Bamm VV, Lanthier DK, Stephenson EL, Smith GST, Harauz G. In vitro study of the direct effect of extracellular hemoglobin on myelin components. Biochim Biophys Acta BBA Mol Basis Dis. 2015;1852(1):92–103.

156. Linsell L, Malouf R, Morris J, Kurinczuk JJ, Marlow N. Prognostic factors for cerebral palsy and motor impairment in children born very preterm or very low birthweight: a systematic review. Dev Med Child Neurol. 2016;58(6):554–69.

157. Gressens P, Richelme C, Kadhim HJ, Gadisseux JF, Evrard P. The germinative zone produces the most cortical astrocytes after neuronal migration in the developing mammalian brain. Biol Neonate. 1992;61(1):4–24.

158. Radonjić NV, Ayoub AE, Memi F, Yu X, Maroof A, Jakovcevski I, et al. Diversity of cortical interneurons in primates: the role of the dorsal proliferative niche. Cell Rep. 2014;9(6):2139–51.

159. Cottrell GT, Ferguson AV. Sensory circumventricular organs: central roles in integrated autonomic regulation. Regul Pept. 2004;117(1):11–23.

160. Moseley ME, Cohen Y, Mintorovitch J, Chileuitt L, Shimizu H, Kucharczyk J, et al. Early detection of regional cerebral ischemia in cats: comparison of diffusion- and T2-weighted MRI and spectroscopy. Magn Reson Med. 1990;14(2):330–46.

161. Warach S, Chien D, Li W, Ronthal M, Edelman RR. Fast magnetic resonance diffusion-weighted imaging of acute human stroke. Neurology. 1992;42(9):1717–23.

162. Bihan DL, Urayama S, Aso T, Hanakawa T, Fukuyama H. Direct and fast detection of neuronal activation in the human brain with diffusion MRI. Proc Natl Acad Sci U S A. 2006;103(21):8263–8.

163. Aso T, Urayama S, Poupon C, Sawamoto N, Fukuyama H, Bihan DL. An intrinsic diffusion response function for analyzing diffusion functional MRI time series. NeuroImage. 2009;47(4):1487–95.

164. Åkerström B, Maghzal GJ, Winterbourn CC, Kettle AJ. The lipocalin α1-microglobulin has radical scavenging activity. J Biol Chem. 2007;282(43):31493–503.

165. Allhorn M, Berggård T, Nordberg J, Olsson ML. Processing of the lipocalin a-1-microglobulin by hemoglobin induces heme-binding and heme-degradation properties. Blood. 2002;99(6):1894–901.

166. Ley D, Romantsik O, Vallius S, Sveinsdóttir K, Sveinsdóttir S, Agyemang AA, et al. High presence of extracellular hemoglobin in the periventricular white matter following preterm intraventricular hemorrhage. Front Physiol. 2016;7:330.

167. Wang Y-C, Wang P-F, Fang H, Chen J, Xiong X-Y, Yang Q-W. Toll-like receptor 4 antagonist attenuates intracerebral hemorrhage–induced brain injury. Stroke. 2013;44(9):2545–52.

168. Garton T, Keep RF, Hua Y, Xi G. CD163, a hemoglobin/haptoglobin scavenger receptor, after intracerebral hemorrhage: functions in microglia/macrophages versus neurons. Transl Stroke Res. 2017;8(6):612–6.

169. Cui H-J, He H, Yang A-L, Zhou H-J, Wang C, Luo J-K, et al. Efficacy of deferoxamine in animal models of intracerebral hemorrhage: a systematic review and stratified meta-analysis. Ai J, editor. PloS One. 2015 May 22;10(5):e0127256.

170. Xie Q, Gu Y, Hua Y, Liu W, Keep RF, Xi G. Deferoxamine attenuates white matter injury in a piglet intracerebral hemorrhage model. Stroke. 2014;45(1):290–2.

171. Selim M, Foster LD, Moy CS, Xi G, Hill MD, Morgenstern LB, et al. Deferoxamine mesylate in patients with intracerebral haemorrhage (i-DEF): a multicentre, randomised, placebo-controlled, double-blind phase 2 trial. Lancet Neurol. 2019;18(5):428–38.

172. Wu Z, Zou X, Zhu W, Mao Y, Chen L, Zhao F. Minocycline is effective in intracerebral hemorrhage by inhibition of apoptosis and autophagy. J Neurol Sci. 2016;371:88–95.

173. Guo J, Chen Q, Tang J, Zhang J, Tao Y, Li L, et al. Minocycline-induced attenuation of iron overload and brain injury after experimental germinal matrix hemorrhage. Brain Res. 2015;1594:115–24.

174. Tang J, Chen Q, Guo J, Yang L, Tao Y, Li L, et al. Minocycline attenuates neonatal germinal-matrix-hemorrhage-induced neuroinflammation and brain edema by activating cannabinoid receptor 2. Mol Neurobiol. 2016;53(3):1935–48.

175. International randomised controlled trial of acetazolamide and furosemide in posthaemorrhagic ventricular dilatation in infancy. The Lancet. 1998 Aug;352(9126):433–40.

176. Kazan S, Güra A, Uçar T, Korkmaz E, Ongun H, Akyuz M. Hydrocephalus after intraventricular hemorrhage in preterm and low–birth weight infants: analysis of associated risk factors for ventriculoperitoneal shunting. Surg Neurol. 2005;64:S77–81.

177. Kennedy CR, Ayers S, Campbell MJ, Elbourne D, Hope P, Johnson A, et al. Randomized, controlled trial of acetazolamide and furosemide in posthemorrhagic ventricular dilation in infancy: follow-up at 1 year. Pediatrics. 2001;108(3):597–607.

178. Zhang H, Fang X, Huang D, Luo Q, Zheng M, Wang K, et al. Erythropoietin signaling increases neurogenesis and oligodendrogenesis of endogenous neural stem cells following spinal cord injury both in vivo and in vitro. Mol Med Rep. 2017;17(1):264–72.

179. Wei S, Luo C, Yu S, Gao J, Liu C, Wei Z, et al. Erythropoietin ameliorates early brain injury after subarachnoid haemorrhage by modulating microglia polarization via the EPOR/JAK2-STAT3 pathway. Exp Cell Res. 2017;361(2):342–52.

180. Robinson S, Conteh FS, Oppong AY, Yellowhair TR, Newville JC, Demerdash NE, et al. Extended combined neonatal treatment with erythropoietin plus melatonin prevents posthemorrhagic hydrocephalus of prematurity in rats. Front Cell Neurosci. 2018;12:322.

181. Tesoriere L, D'Arpa D, Conti S, Giaccone V, Pintaudi AM, Livrea MA. Melatonin protects human red blood cells from oxidative hemolysis: New insights into the radical-scavenging activity. J Pineal Res. 1999;27(2):95–105.

182. Hayter CL, Bishop GM, Robinson SR. Pharmacological but not physiological concentrations of melatonin reduce iron-induced neuronal death in rat cerebral cortex. Neurosci Lett. 2004;362(3):182–4.

183. Ahn SY, Chang YS, Sung SI, Park WS. Mesenchymal stem cells for severe intraventricular hemorrhage in preterm infants: phase I dose-escalation clinical trial: mesenchymal stem cells for neonatal IVH. STEM CELLS Transl Med. 2018;7(12):847–56.

184. Park WS, Sung SI, Ahn SY, Sung DK, Im GH, Yoo HS, et al. Optimal timing of mesenchymal stem cell therapy for neonatal intraventricular hemorrhage. Cell Transplant. 2016;25(6):1131–44.

185. Nonaka M, Yoshikawa M, Nishimura F, Yokota H, Kimura H, Hirabayashi H, et al. Intraventricular transplantation of embryonic stem cell-derived neural stem cells in intracerebral hemorrhage rats. Neurol Res. 2004;26(3):265–72.

186. Ley D, Hallberg B, Hansen-Pupp I, Dani C, Ramenghi LA, Marlow N, et al. rhIGF-1/rhIGFBP-3 in preterm infants: a phase 2 randomized controlled trial. J Pediatr. 2019;206:56-65.e8.

187. Beijst C, Dudink J, Wientjes R, Benavente-Fernandez I, Groenendaal F, Brouwer MJ. Two-dimensional ultrasound measurements vs. magnetic resonance imaging-derived ventricular volume of preterm infants with germinal matrix intraventricular haemorrhage. Pediatr Radiol. 2020;50(2):234–41.

188. Horsch S, Bengtsson J, Nordell A, Lagercrantz H, Ådén U, Blennow M. Lateral ventricular size in extremely premature infants: 3D MRI confirms 2D ultrasound measurements. Ultrasound Med Biol. 2009;35(3):360–6.

189. Batton DG, Swails TL. Isolated lateral ventricular asymmetry in very low-birth-weight infants: a left-sided lesion? Am J Perinatol. 1998;15(3):183–6.

190. Health C for D and R. Marketing Clearance of Diagnostic Ultrasound Systems and Transducers [Internet]. U.S. Food and Drug Administration. FDA; 2019. Available from: https://www.fda.gov/regulatory-information/search-fda-guidance-documents/marketing-clearance-diagnostic-ultrasound-systems-and-transducers

191. Koo TK, Li MY. A guideline of selecting and reporting intraclass correlation coefficients for reliability research. J Chiropr Med. 2016;15(2):155–63.

192. Whitaker AH, Van Rossem R, Feldman JF, Schonfeld IS, Pinto-Martin JA, Tore C, et al. Psychiatric outcomes in low-birth-weight children at age 6 years: relation to neonatal cranial ultrasound abnormalities. Arch Gen Psychiatry. 1997;54(9):847–56.

193. Movsas TZ, Pinto-Martin JA, Whitaker AH, Feldman JF, Lorenz JM, Korzeniewski SJ, et al. Autism spectrum disorder is associated with ventricular enlargement in a low birth weight population. J Pediatr. 2013;163(1):73–8.

194. Boghossian NS, Geraci M, Edwards EM, Horbar JD. Sex differences in mortality and morbidity of infants born at less than 30 weeks' gestation. Pediatrics. 2018;142(6):e20182352.

195. Ardalan M, Svedin P, Baburamani AA, Supramaniam VG, Ek J, Hagberg H, et al. Dysmaturation of somatostatin interneurons following umbilical cord occlusion in preterm fetal sheep. Front Physiol. 2019;10:563.

Cerebral intraventricular hemorrhage and post-hemorrhagic ventricular dilatation in preterm infants

The inspiration for this thesis comes from my everyday clinical practice facing tiny babies and their families. One in 10 babies is born prematurely (before 37 weeks of completed pregnancy) every year worldwide. Cerebral intraventricular hemorrhage is serious comorbidity of prematurity, affecting nearly 1/3 of very preterm infants. Currently, cerebral intraventricular hemorrhage is neither preventable nor treatable.

This thesis gives insights into new pathophysiological mechanisms and potential treatment strategies for cerebral intraventricular hemorrhage.

"No problem is insurmountable. With a little courage, teamwork, and determination a person can overcome anything".

Louisa May Alcott.

FACULTY OF MEDICINE

LUND UNIVERSITY